US011181499B2

(12) **United States Patent**
Abdolahad et al.

(10) **Patent No.: US 11,181,499 B2**
(45) **Date of Patent: *Nov. 23, 2021**

(54) **REAL-TIME AND LABEL FREE ANALYZER FOR IN-VITRO AND IN-VIVO DETECTING OF CANCER**

(71) Applicants: **Mohammad Abdolahad**, Tehran (IR); **Zohreh Sadat Miripour**, Tehran (IR); **Sahar NajafiKhoshnoo**, Tehran (IR)

(72) Inventors: **Mohammad Abdolahad**, Tehran (IR); **Zohreh Sadat Miripour**, Tehran (IR); **Sahar NajafiKhoshnoo**, Tehran (IR)

(73) Assignee: **NANO HESGARSAZAN SALAMAT ARYA**, Tehran (IR)

(*) Notice: Subject to any disclaimer, the term of this patent is extended or adjusted under 35 U.S.C. 154(b) by 375 days.

This patent is subject to a terminal disclaimer.

(21) Appl. No.: **16/010,510**

(22) Filed: **Jun. 17, 2018**

(65) **Prior Publication Data**

US 2018/0299401 A1 Oct. 18, 2018

Related U.S. Application Data

(60) Provisional application No. 62/522,115, filed on Jun. 20, 2017, provisional application No. 62/563,673, filed on Sep. 27, 2017.

(51) **Int. Cl.**

A61B 5/05	(2021.01)
G01N 27/327	(2006.01)

(Continued)

(52) **U.S. Cl.**

CPC ***G01N 27/3278*** (2013.01); ***A61B 5/14735*** (2013.01); ***A61B 5/6849*** (2013.01); ***G01N 27/48*** (2013.01); ***G01N 33/4833*** (2013.01); *A61B 2562/0285* (2013.01); *A61B 2562/046* (2013.01); *G01N 27/3277* (2013.01)

(58) **Field of Classification Search**

CPC G01N 27/3278; G01N 27/48; G01N 33/4833; G01N 27/3277; A61B 5/14735; A61B 5/6849; A61B 2562/046; A61B 2562/0285

See application file for complete search history.

(56) **References Cited**

U.S. PATENT DOCUMENTS

7,939,734 B1 *	5/2011	Li	G01N 27/3277	435/6.1
2009/0061451 A1 *	3/2009	Achim	G01N 33/5438	435/6.11

(Continued)

OTHER PUBLICATIONS

Wikipedia contributors. "American wire gauge." Wikipedia, The Free Encyclopedia, https://web.archive.org/web/20071103232133/http://en.wikipedia.org:80/wiki/American_wire_gauge#Table_of_AWGs_and_approximate_corresponding_sizes, Nov. 3, 2007. Accessed Oct. 29, 2020 (Year: 2007).*

Primary Examiner — Andrey Shostak
(74) *Attorney, Agent, or Firm* — Bajwa IP Law Firm; Haris Zaheer Bajwa

(57) **ABSTRACT**

An electrochemical system for cancer diagnosis. The electrochemical system includes a sensor configured to be put in contact with a sample suspected to be cancerous, an electrochemical stimulator-analyzer, a processor electrically connected to the electrochemical stimulator-analyzer, and an array of electrically conductive connectors connecting the sensor to the electrochemical stimulator-analyzer.

8 Claims, 44 Drawing Sheets

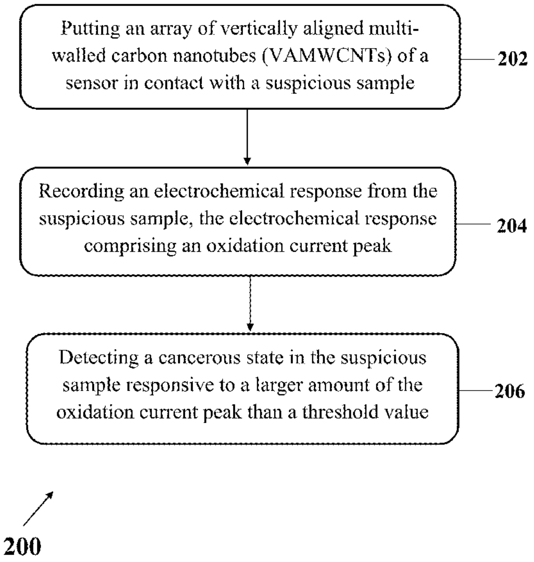

(51) **Int. Cl.**

G01N 27/48	(2006.01)
A61B 5/1473	(2006.01)
A61B 5/00	(2006.01)
G01N 33/483	(2006.01)

(56) **References Cited**

U.S. PATENT DOCUMENTS

2009/0076496	A1*	3/2009	Azure	A61B 18/1485 606/34
2015/0268207	A1*	9/2015	Motayed	G01N 33/0031 506/13

* cited by examiner

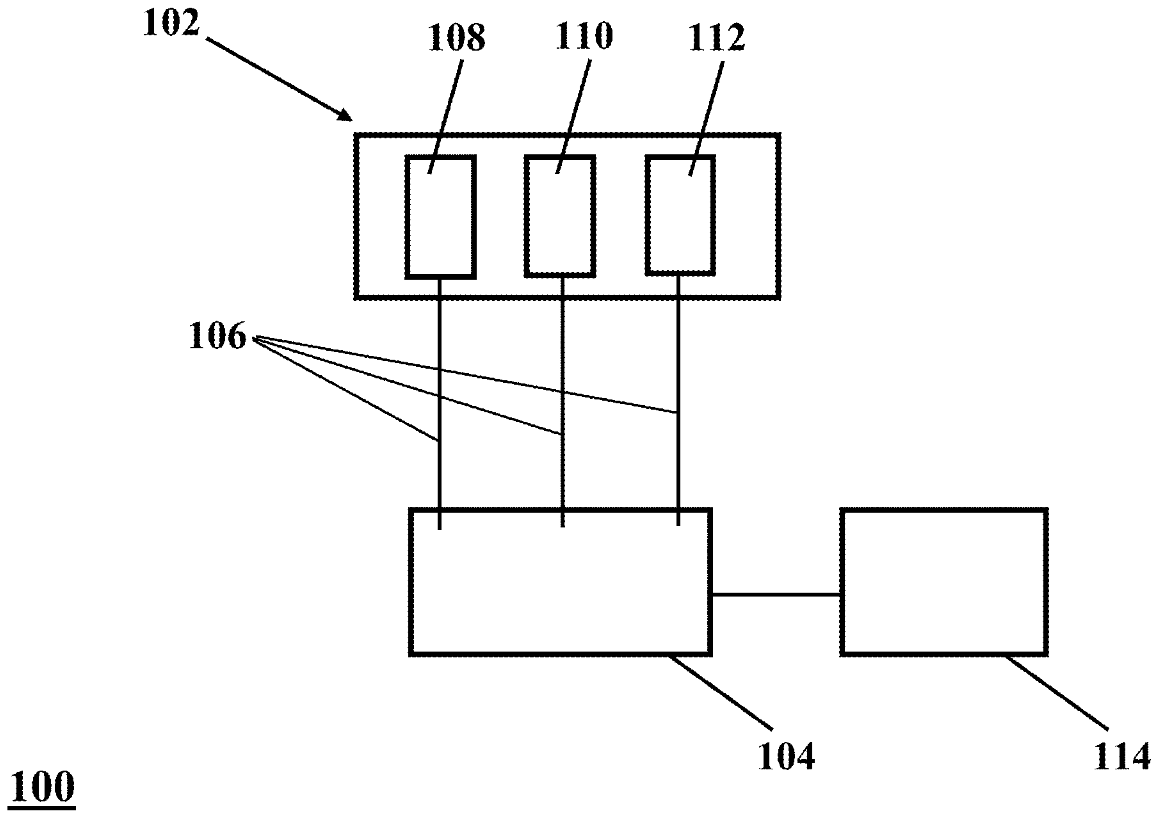

FIG. 1A

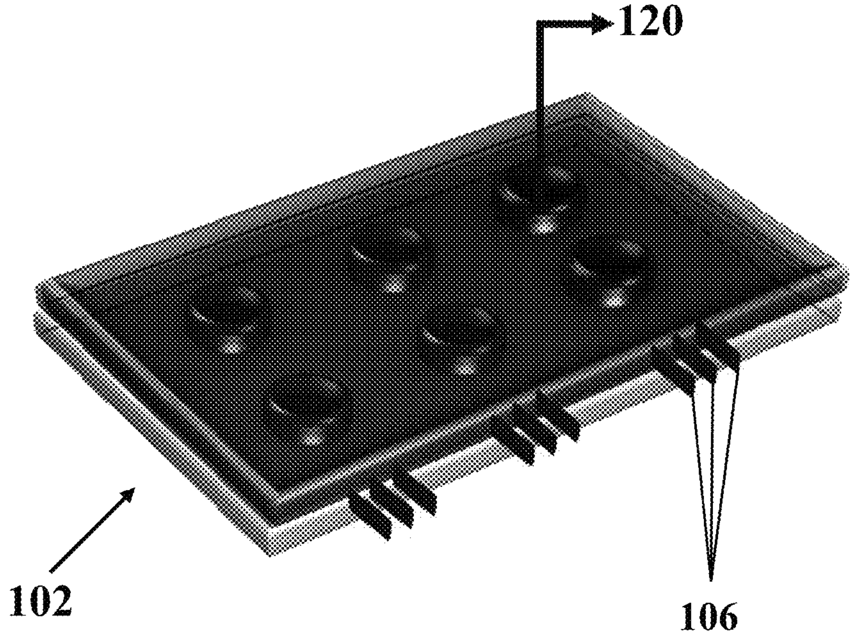

FIG. 1B

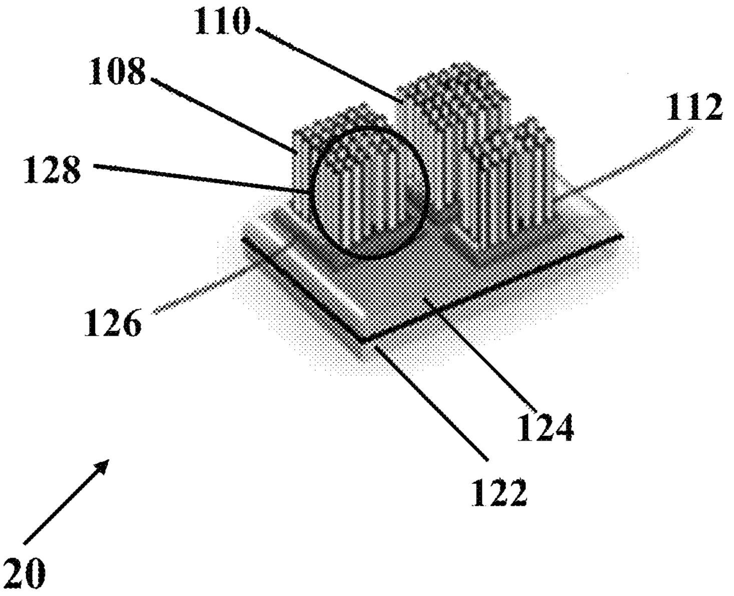

FIG. 1C

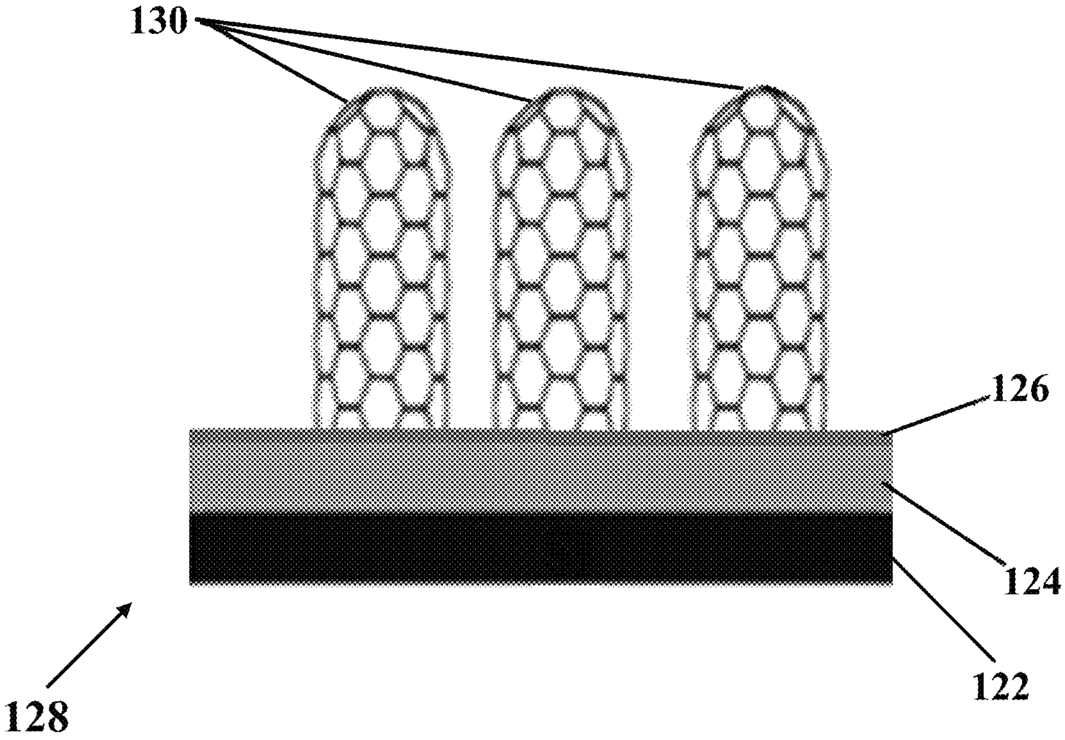

FIG. 1D

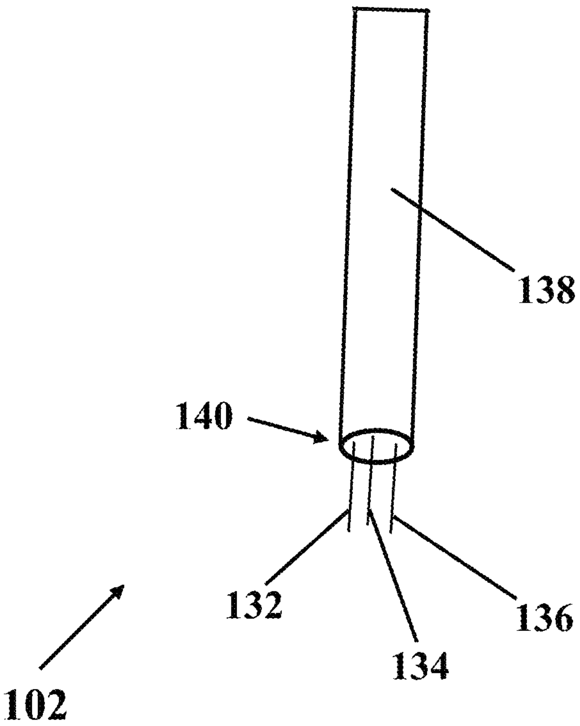

FIG. 1E

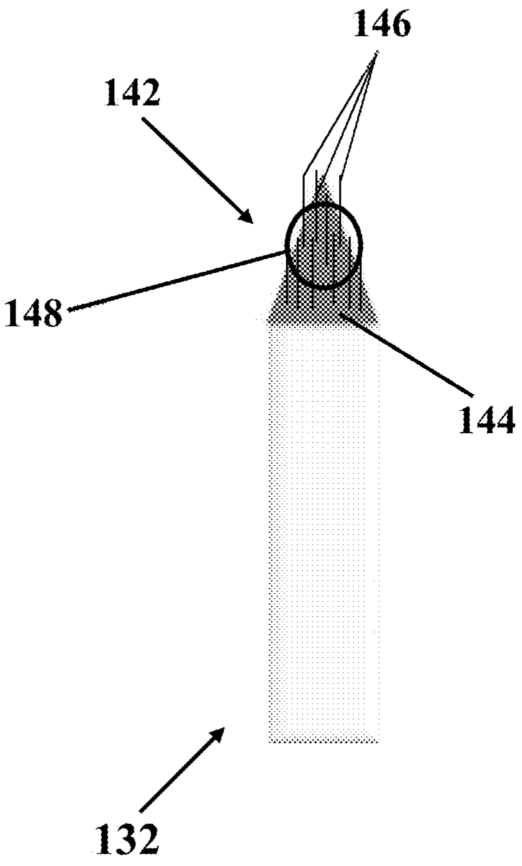

FIG. 1F

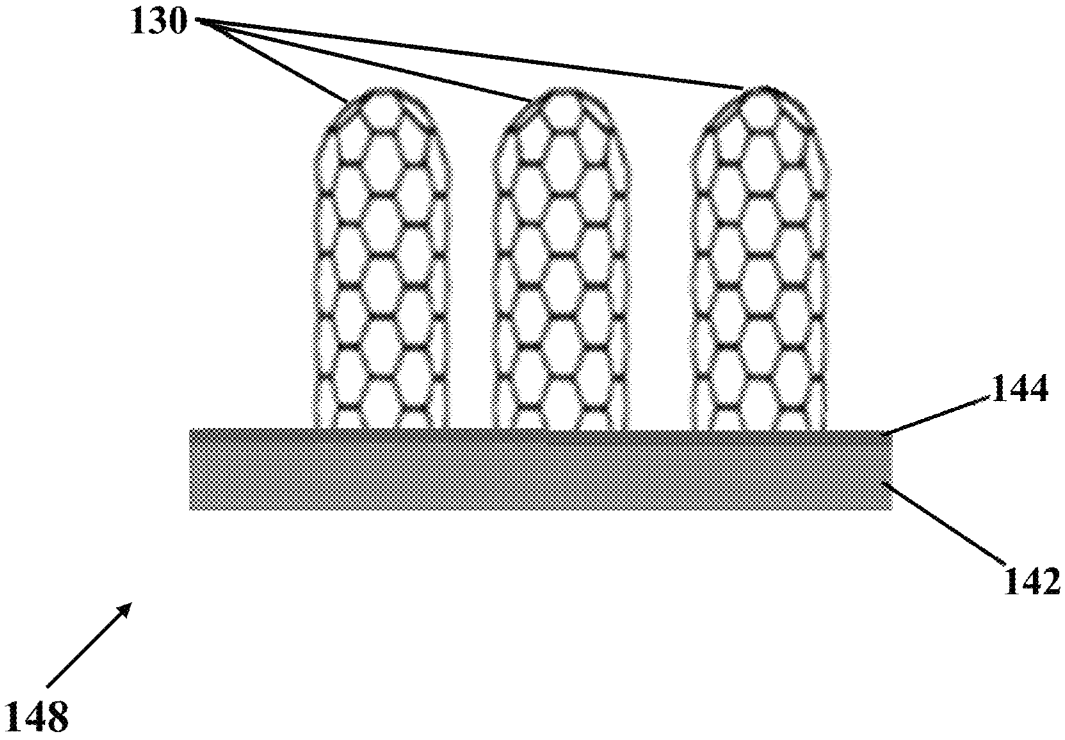

FIG. 1G

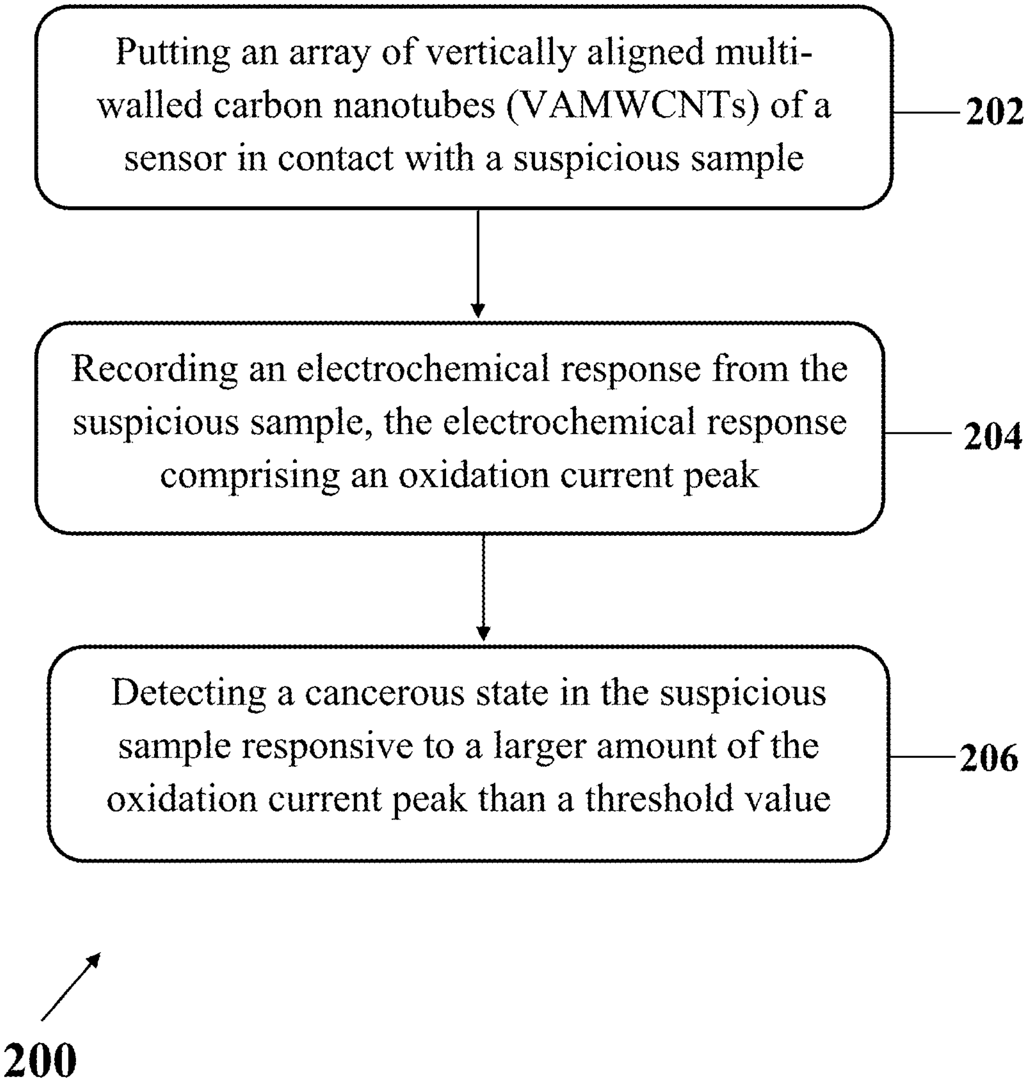
Putting an array of vertically aligned multi-walled carbon nanotubes (VAMWCNTs) of a sensor in contact with a suspicious sample
202
Recording an electrochemical response from the suspicious sample, the electrochemical response comprising an oxidation current peak
204
Detecting a cancerous state in the suspicious sample responsive to a larger amount of the oxidation current peak than a threshold value
206
200

FIG. 2A

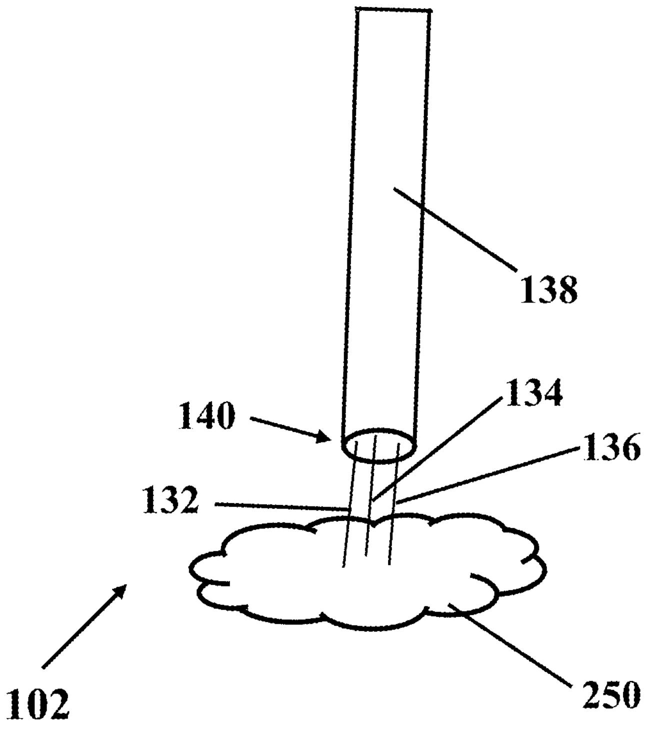

FIG. 2B

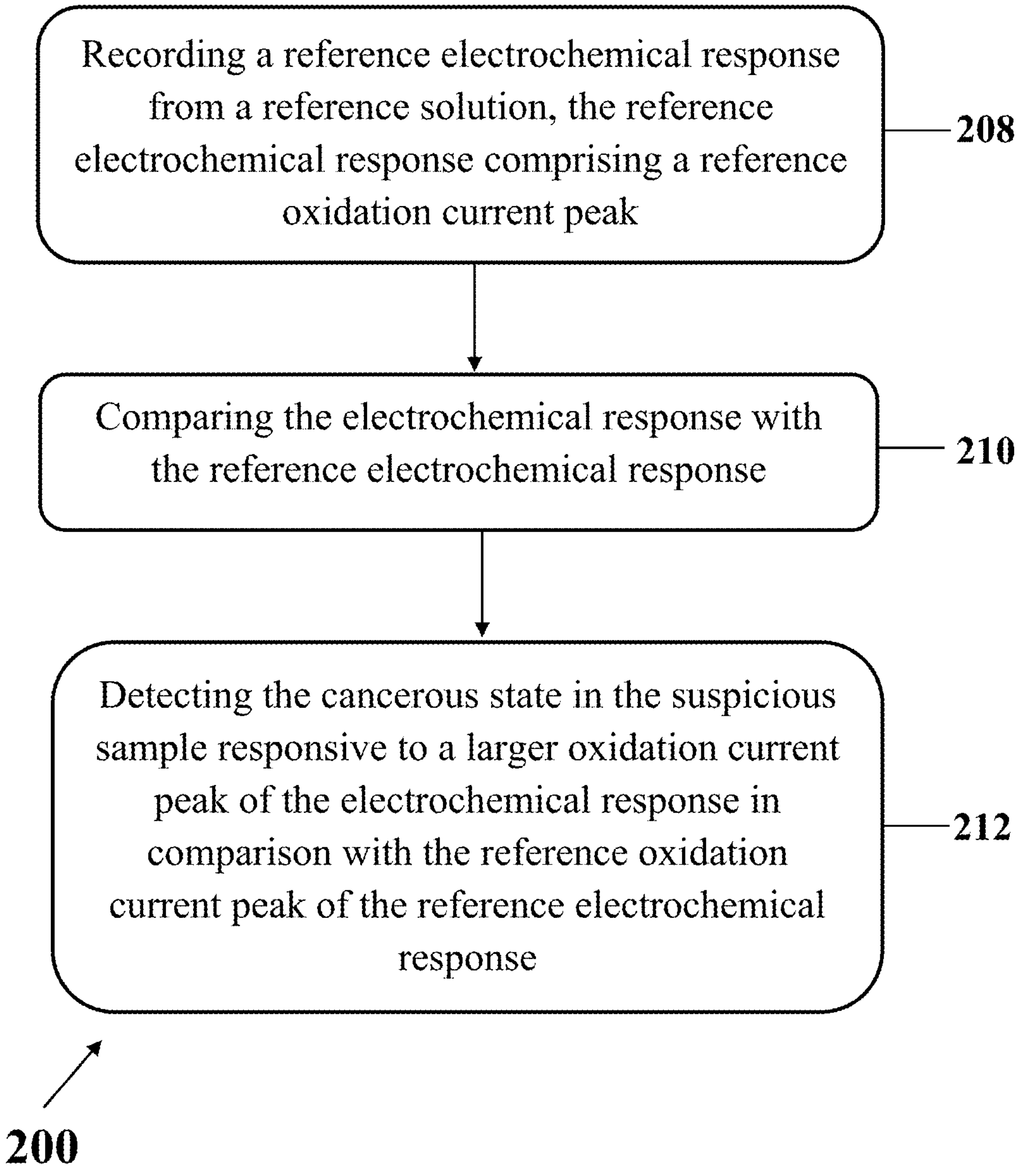
Recording a reference electrochemical response from a reference solution, the reference electrochemical response comprising a reference oxidation current peak
208
Comparing the electrochemical response with the reference electrochemical response
210
Detecting the cancerous state in the suspicious sample responsive to a larger oxidation current peak of the electrochemical response in comparison with the reference oxidation current peak of the reference electrochemical response
212
200

FIG. 2C

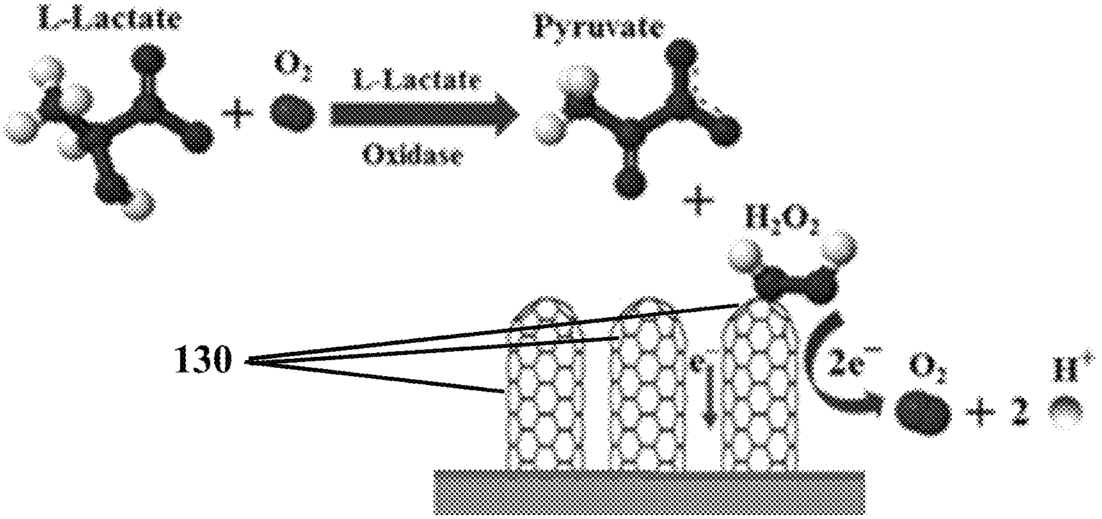

FIG. 3A

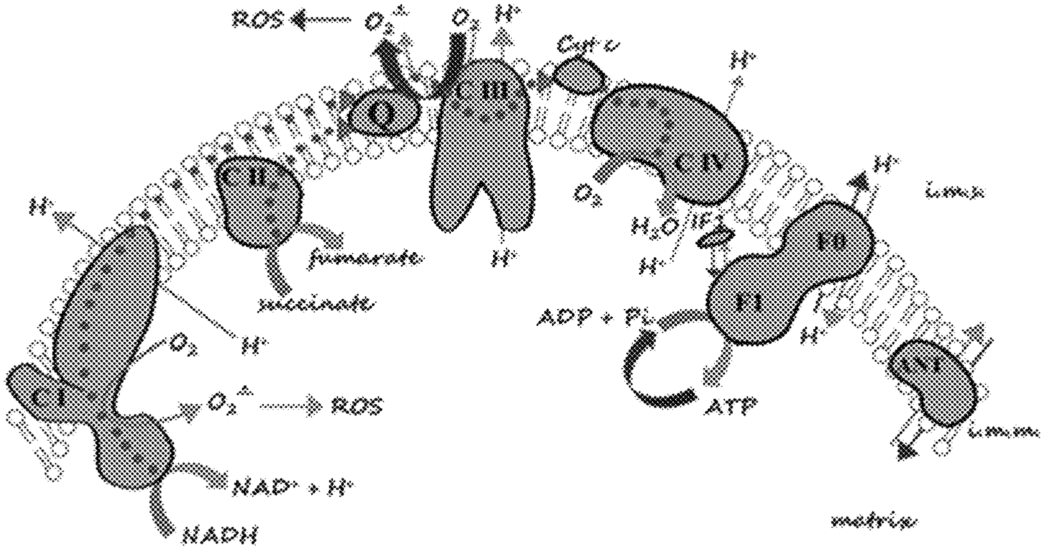
ROS
O2
O2
H+
Cyt c
Q
C III
H+
C II
C IV
ims
O2
H2O
IF1
H+
F0
H+
fumarate
H+
succinate
F1
ADP + Pi
H+
H+
O2
C I
O2
ROS
ATP
ANT
imm
NAD+ + H+
NADH
matrix

FIG. 3B

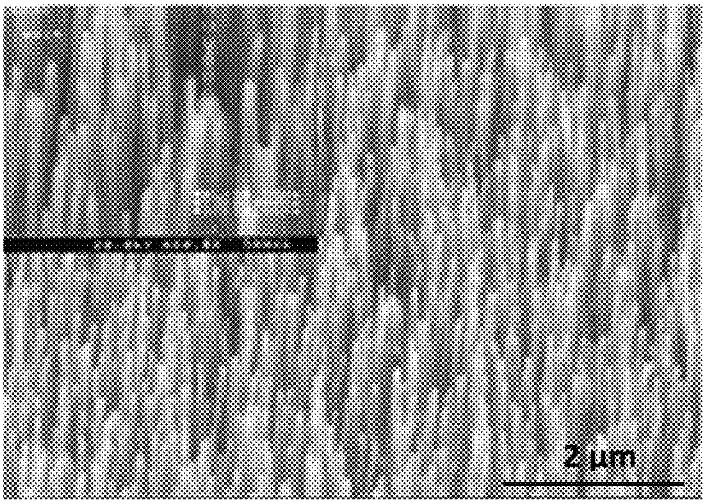

FIG. 4

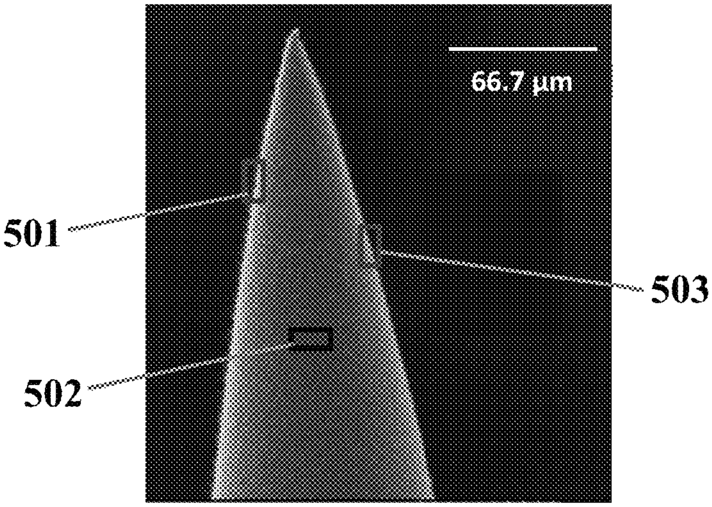

FIG. 5A

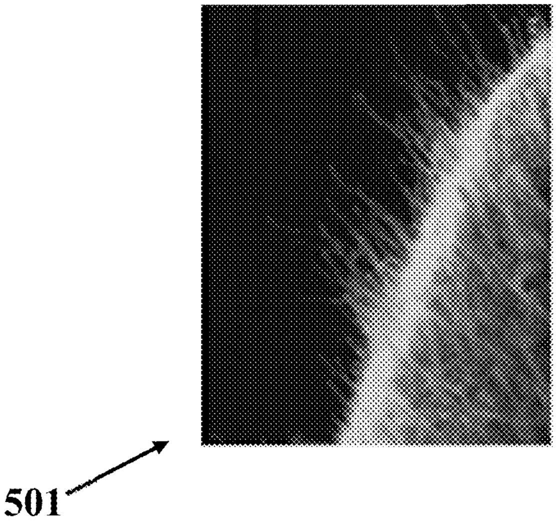

FIG. 5B

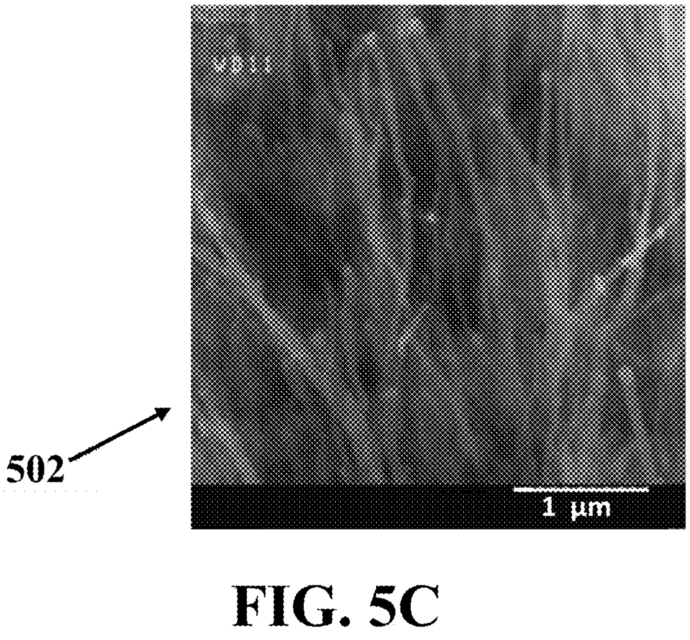

FIG. 5C

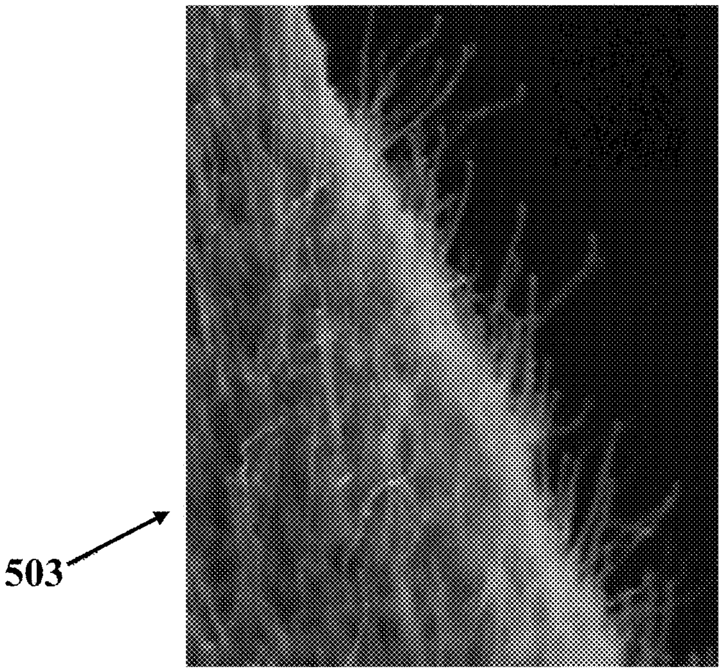

FIG. 5D

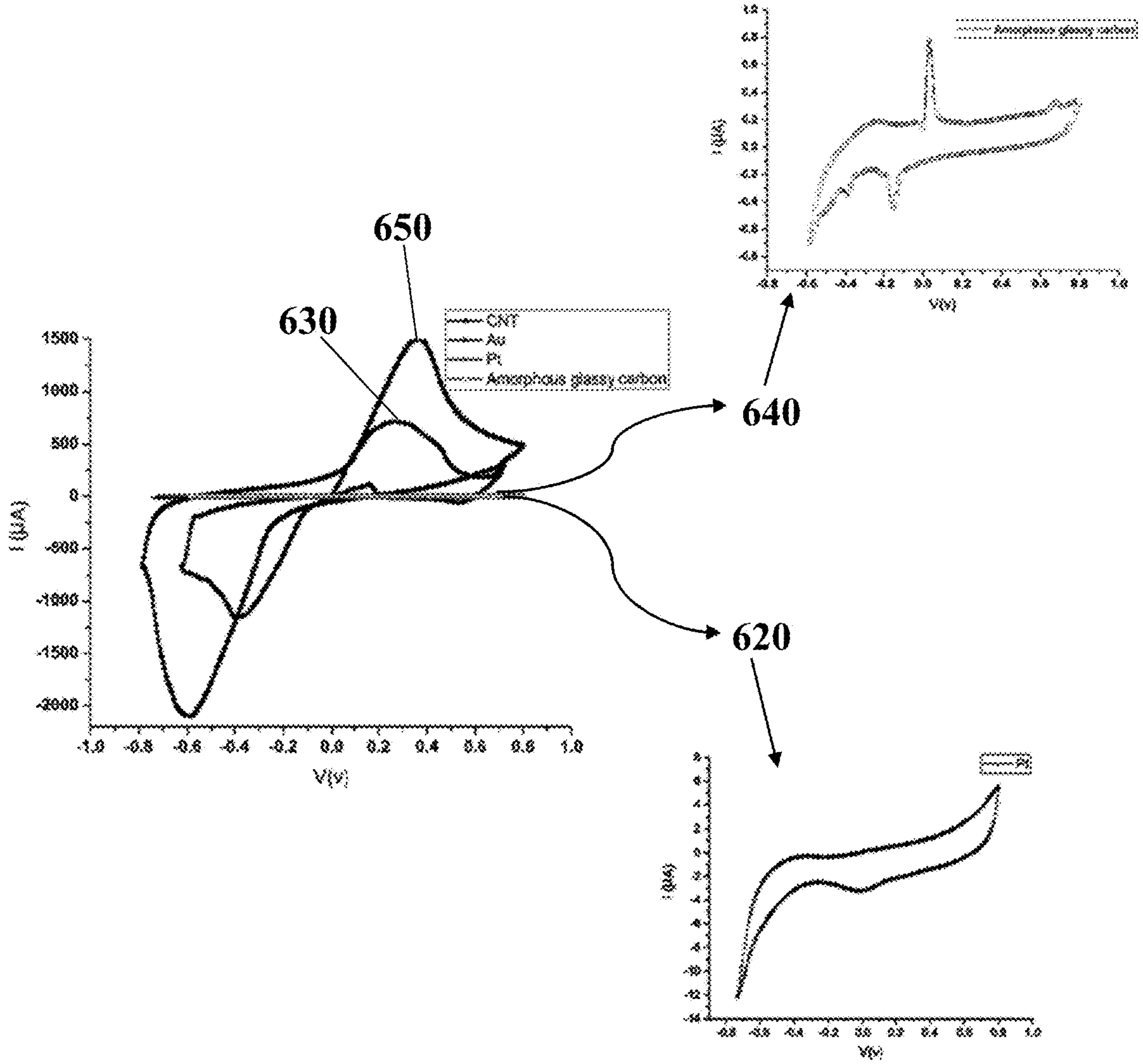
650
630
640
620
CNT
Au
Pt
Amorphous glassy carbon
1500
1000
500
0
-500
-1000
-1500
-2000
I (μA)
-1.0
-0.8
-0.6
-0.4
-0.2
0.0
0.2
0.4
0.6
0.8
1.0
V(v)
Amorphous glassy carbon
1.0
0.8
0.6
0.4
0.2
0.0
-0.2
-0.4
-0.6
-0.8
I (μA)
-0.8
-0.6
-0.4
-0.2
0.0
0.2
0.4
0.6
0.8
1.0
V(v)
Pt
8
6
4
2
0
-2
-4
-6
-8
-10
-12
-14
I (μA)
-0.8
-0.6
-0.4
-0.2
0.0
0.2
0.4
0.6
0.8
1.0
V(v)

FIG. 6A

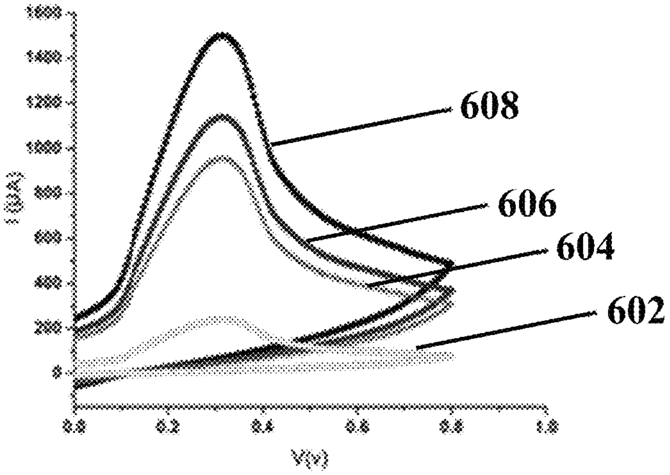
1600
1400
1200
1000
800
600
400
200
0
I (μA)
0.0
0.2
0.4
0.6
0.8
1.0
V(v)
608
606
604
602

FIG. 6B

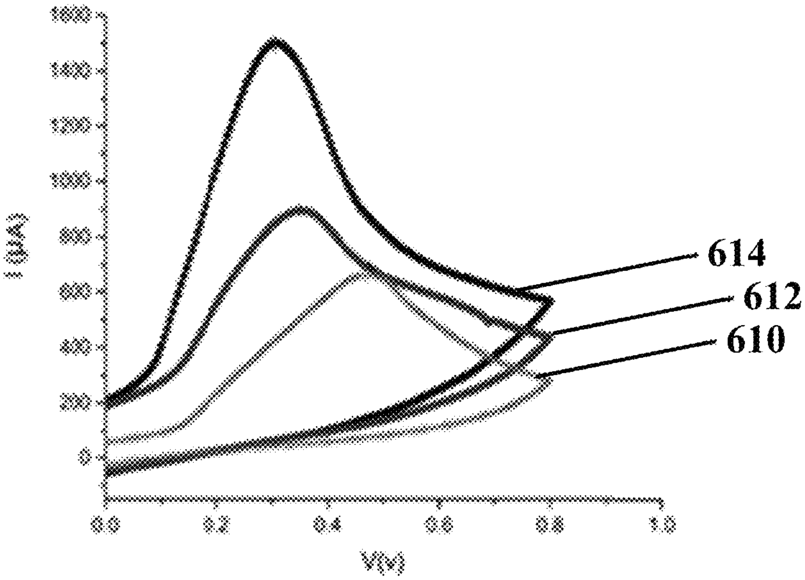
1600
1400
1200
1000
800
600
400
200
0
I (μA)
0.0
0.2
0.4
0.6
0.8
1.0
V(v)
614
612
610

FIG. 6C

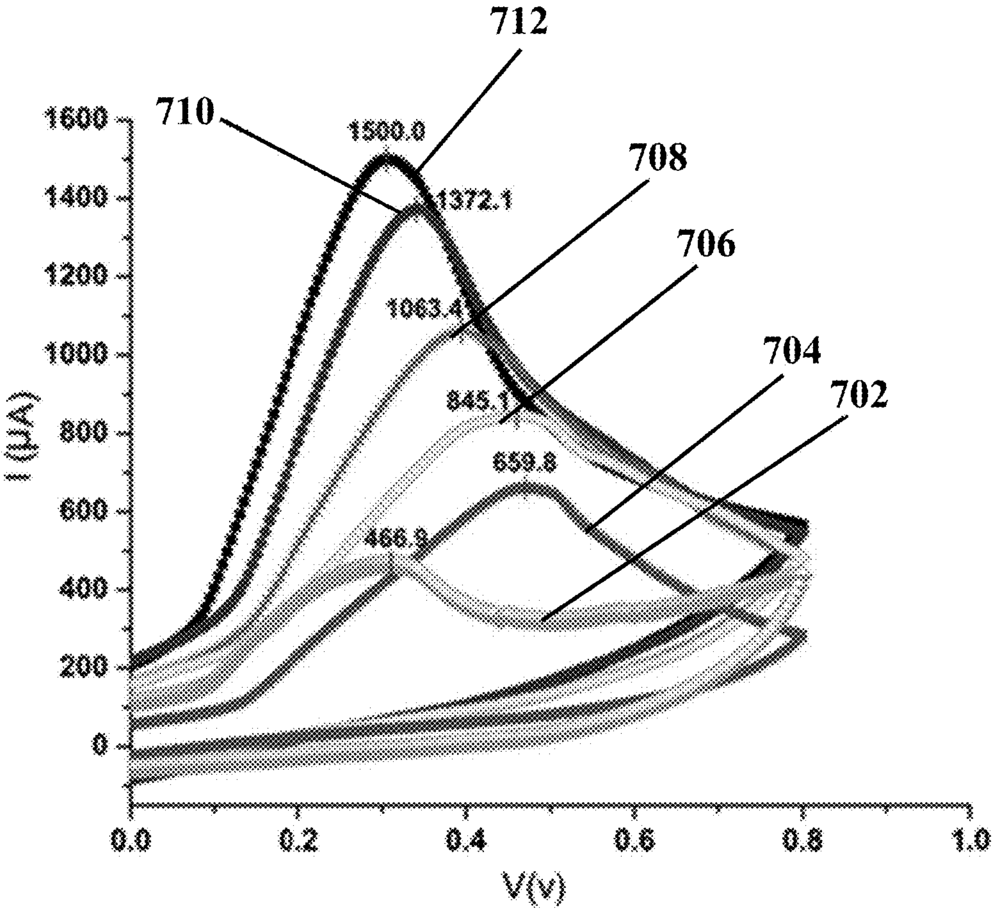
712
710
708
706
704
702
1500.0
1372.1
1063.4
845.1
659.8
466.9
1600
1400
1200
1000
800
600
400
200
0
I (μA)
0.0
0.2
0.4
0.6
0.8
1.0
V(v)

FIG. 7

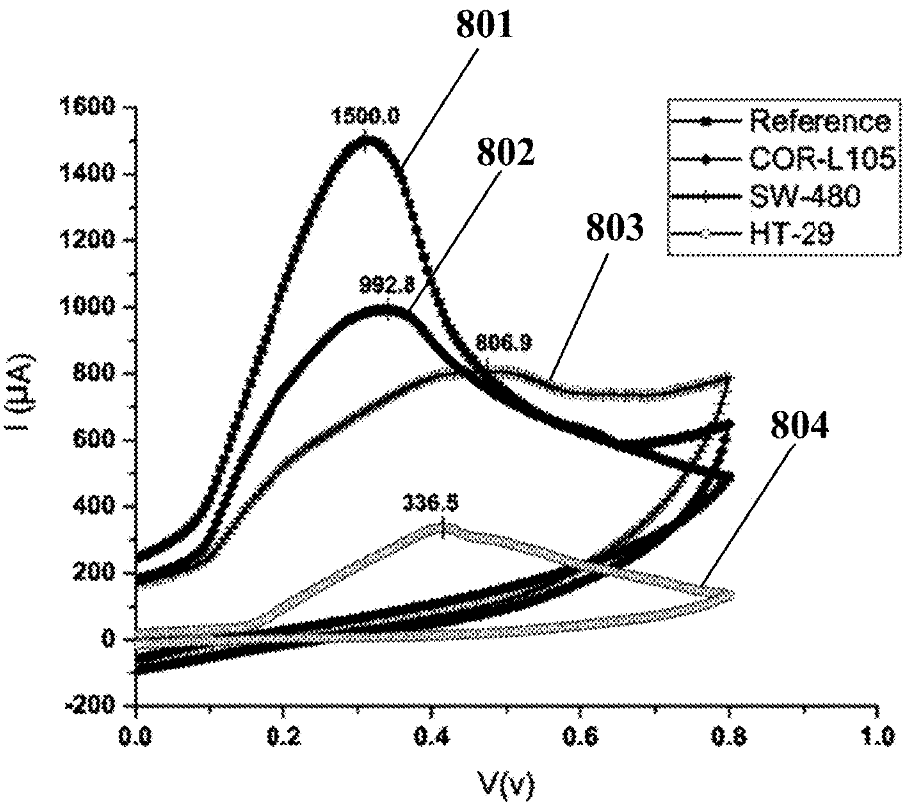
801
802
803
804
1500.0
992.8
806.9
336.5
Reference
COR-L105
SW-480
HT-29
I (μA)
V(v)
1600
1400
1200
1000
800
600
400
200
0
-200
0.0
0.2
0.4
0.6
0.8
1.0

FIG. 8A

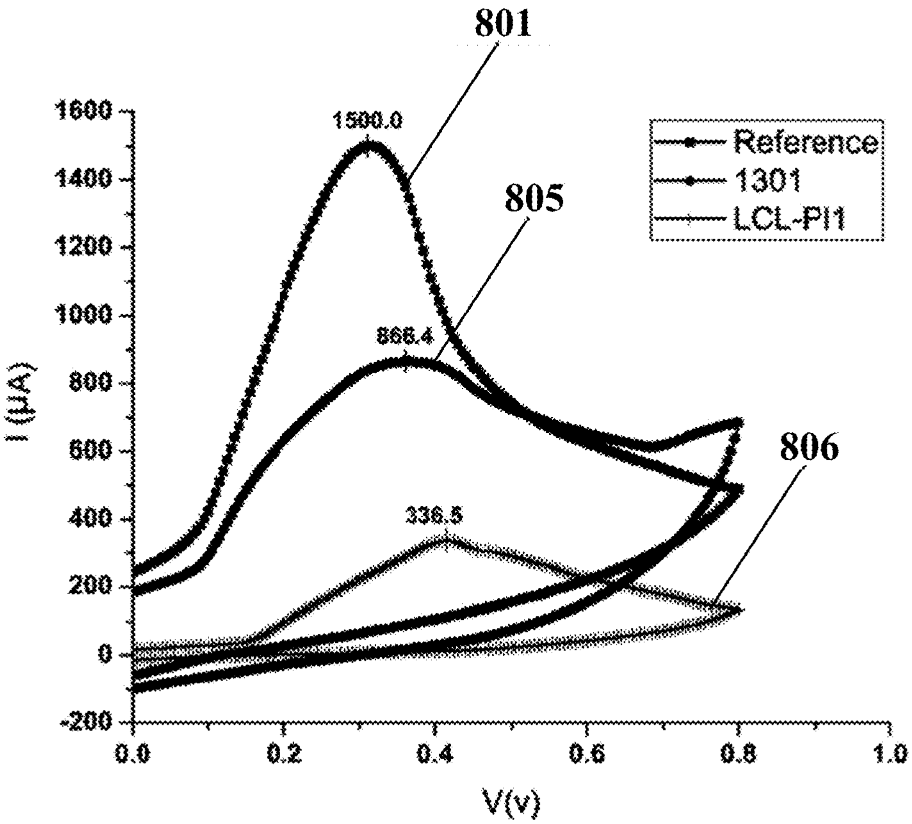
801
805
806
1500.0
868.4
336.5
Reference
1301
LCL-PI1
I (μA)
1600
1400
1200
1000
800
600
400
200
0
-200
0.0
0.2
0.4
0.6
0.8
1.0
V(v)

FIG. 8B

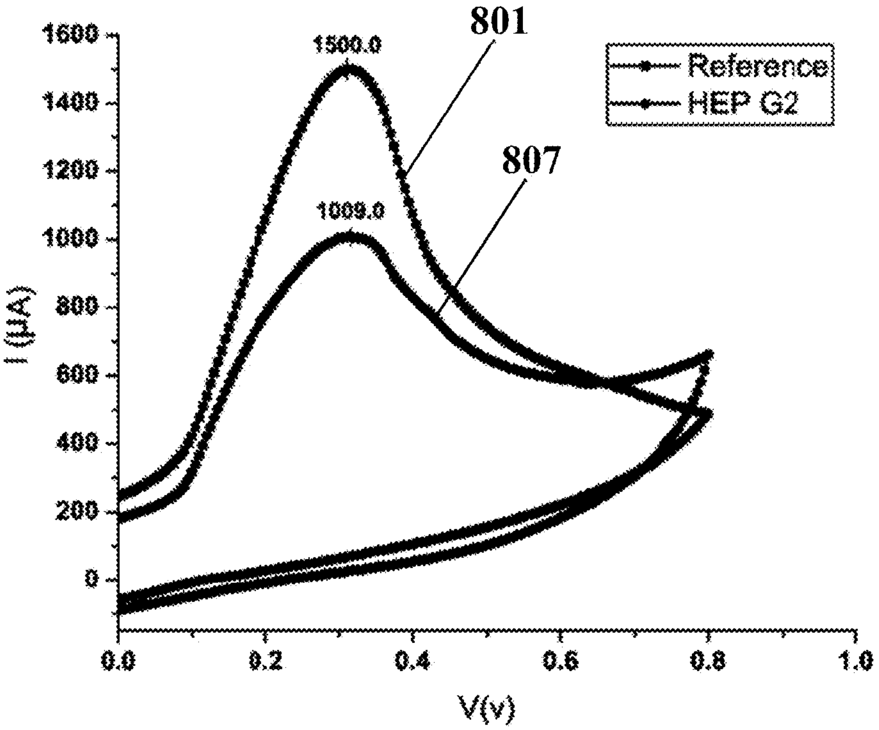
801
807
1500.0
1009.0
Reference
HEP G2
1600
1400
1200
1000
800
600
400
200
0
I (μA)
0.0
0.2
0.4
0.6
0.8
1.0
V(v)

FIG. 8C

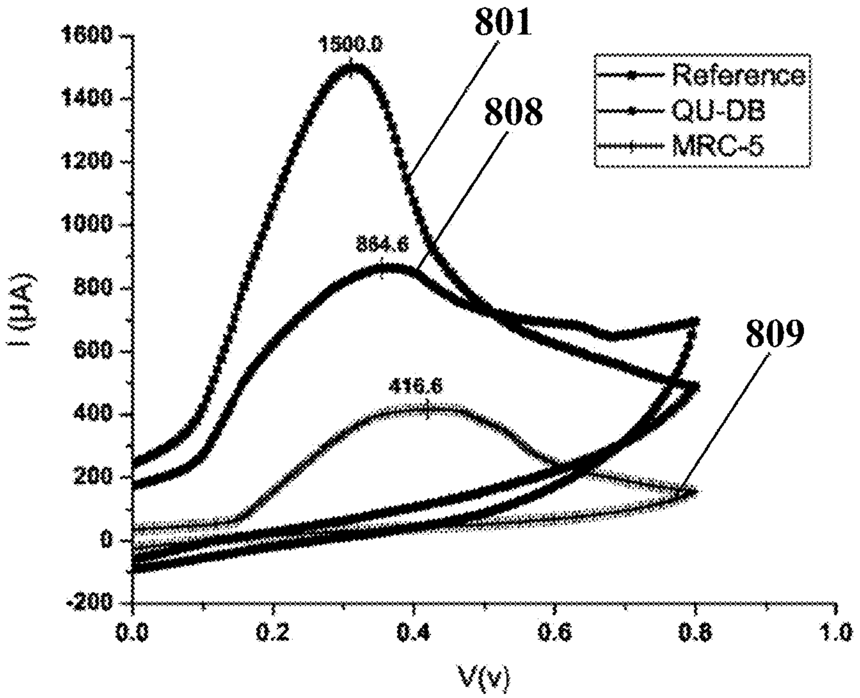
801
808
809
Reference
QU-DB
MRC-5
1500.0
864.6
416.6
1600
1400
1200
1000
800
600
400
200
0
-200
I (μA)
0.0
0.2
0.4
0.6
0.8
1.0
V(v)

FIG. 8D

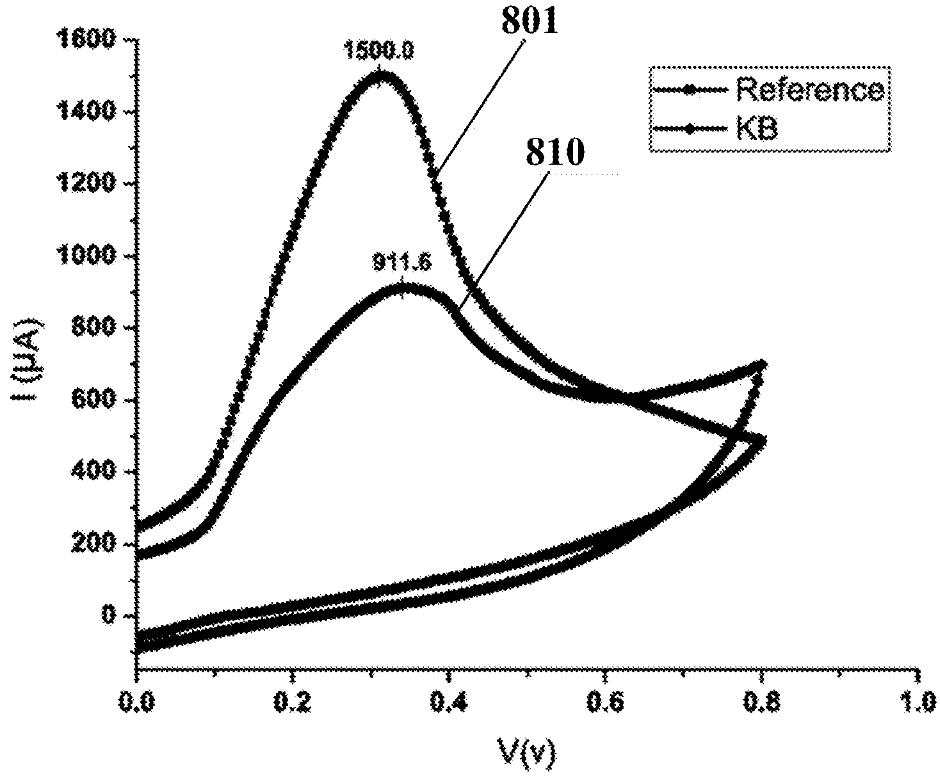
801
810
1500.0
911.6
Reference
KB
I (μA)
V(v)
1600
1400
1200
1000
800
600
400
200
0
0.0
0.2
0.4
0.6
0.8
1.0

FIG. 8E

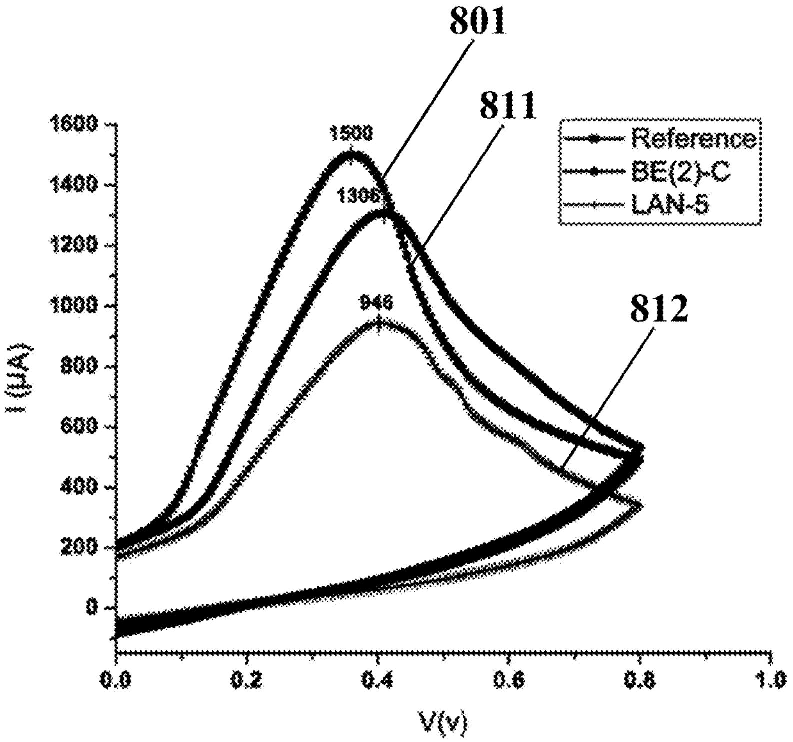
801
811
812
Reference
BE(2)-C
LAN-5
1500
1306
946
1600
1400
1200
1000
800
600
400
200
0
I (μA)
0.0
0.2
0.4
0.6
0.8
1.0
V(v)

FIG. 8F

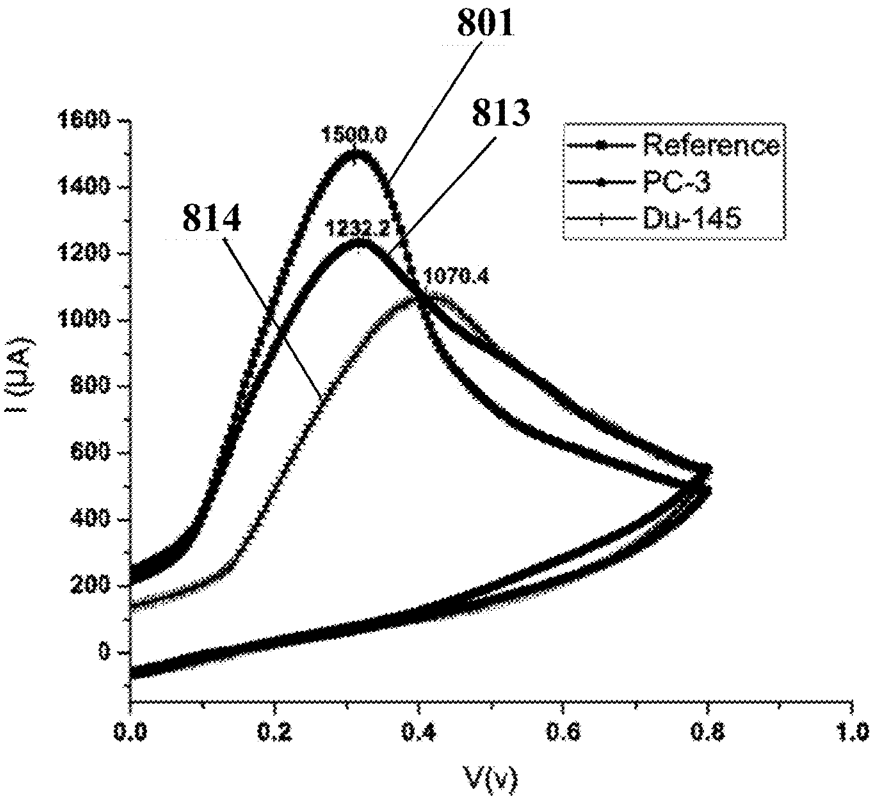
801
813
814
1500.0
1232.2
1070.4
Reference
PC-3
Du-145
I (μA)
1600
1400
1200
1000
800
600
400
200
0
0.0
0.2
0.4
0.6
0.8
1.0
V(v)

FIG. 8G

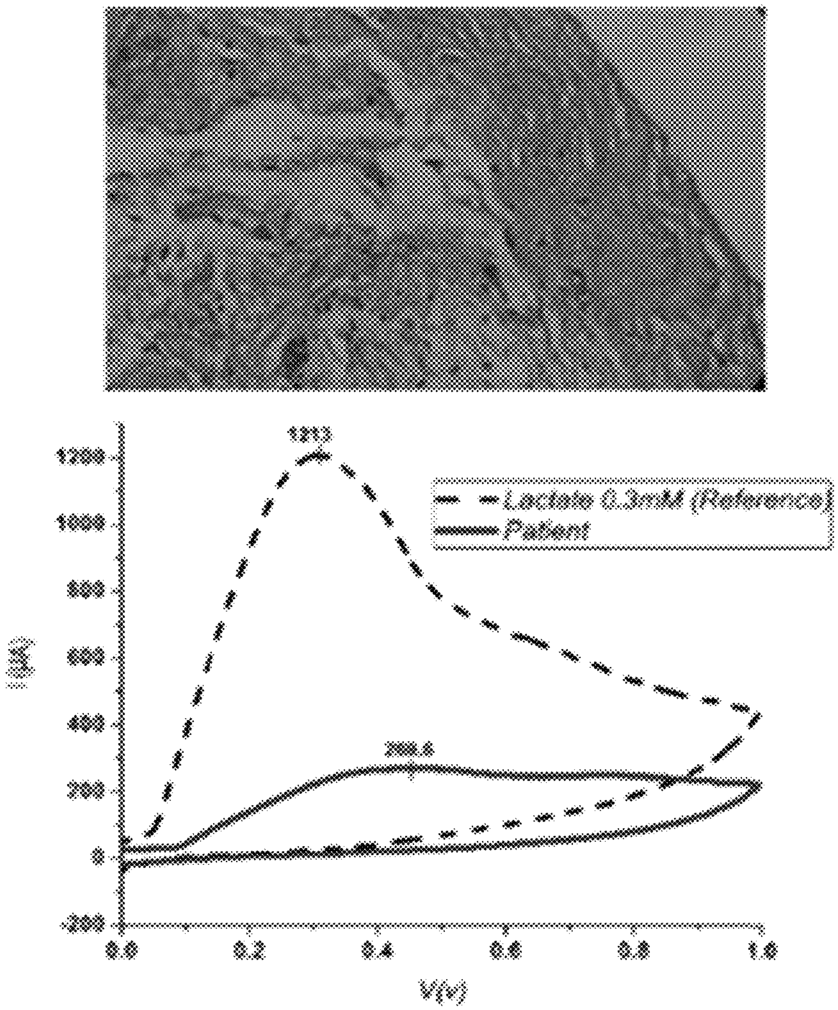
1213
Lactate 0.3mM (Reference)
Patient
268.6
I (µA)
1200
1000
800
600
400
200
0
-200
0.0
0.2
0.4
0.6
0.8
1.0
V(v)

FIG. 9A

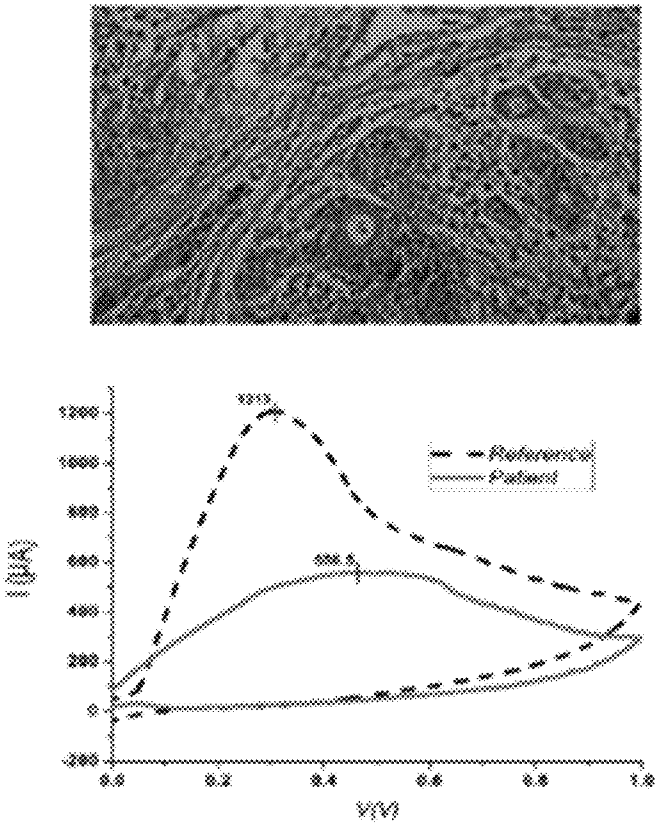
1213
556.5
Reference
Patient
1200
1000
800
600
400
200
0
-200
I (μA)
0.0
0.2
0.4
0.6
0.8
1.0
V(V)

FIG. 9B

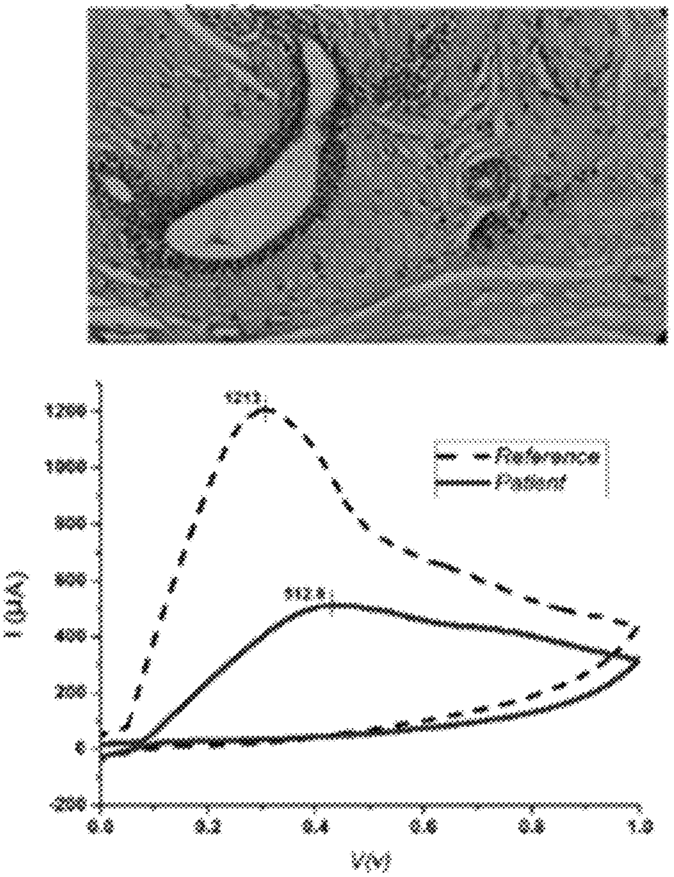
1213
512.8
Reference
Patient
I (μA)
1200
1000
800
600
400
200
0
-200
0.0
0.2
0.4
0.6
0.8
1.0
V(v)

FIG. 9C

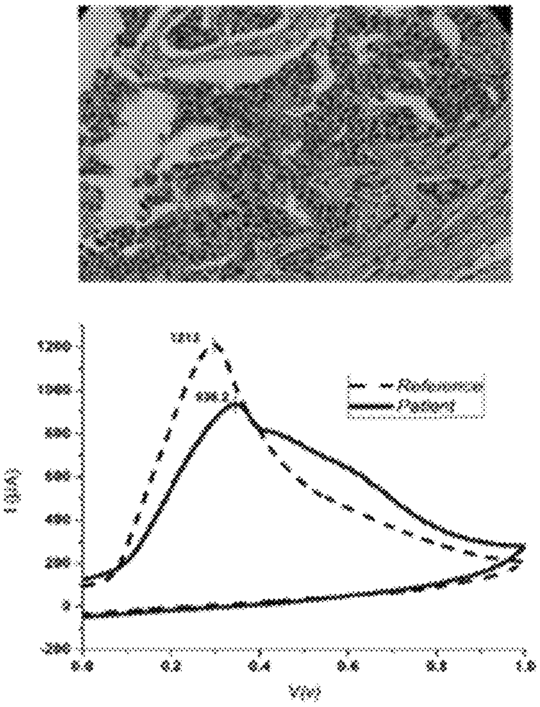
1212
936.2
Reference
Patient
1200
1000
800
600
400
200
0
-200
I (μA)
0.0
0.2
0.4
0.6
0.8
1.0
V(v)

FIG. 9D

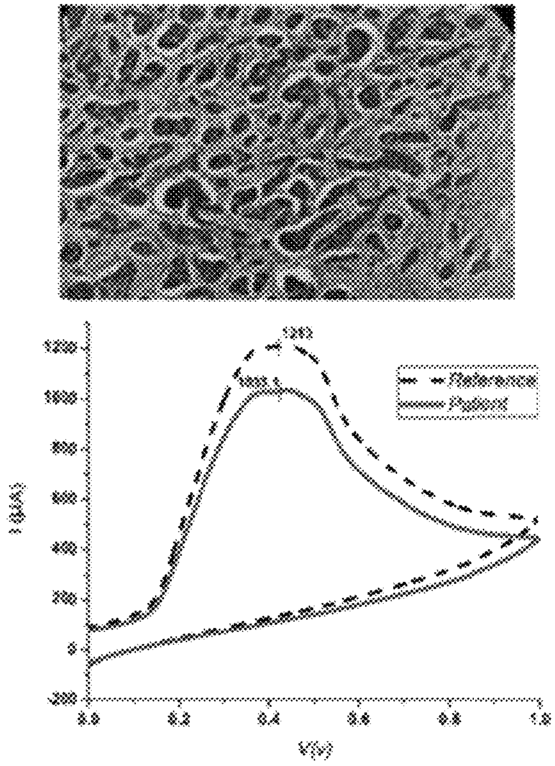
1213
Reference
Patient
1200
1000
800
600
400
200
0
-200
I (μA)
0.0
0.2
0.4
0.6
0.8
1.0
V(v)

FIG. 9E

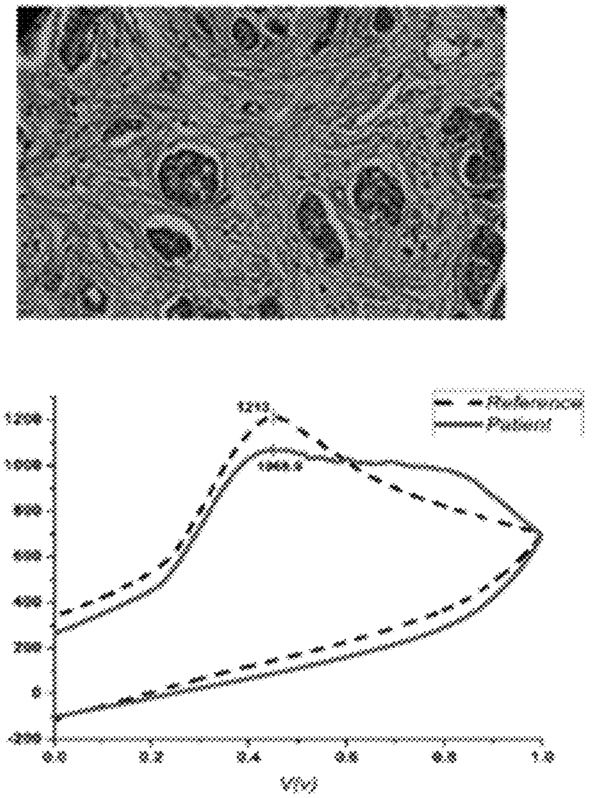
1213
1068.6
Reference
Patient
1200
1000
800
600
400
200
0
-200
I(μA)
0.0
0.2
0.4
0.6
0.8
1.0
V(v)

FIG. 9F

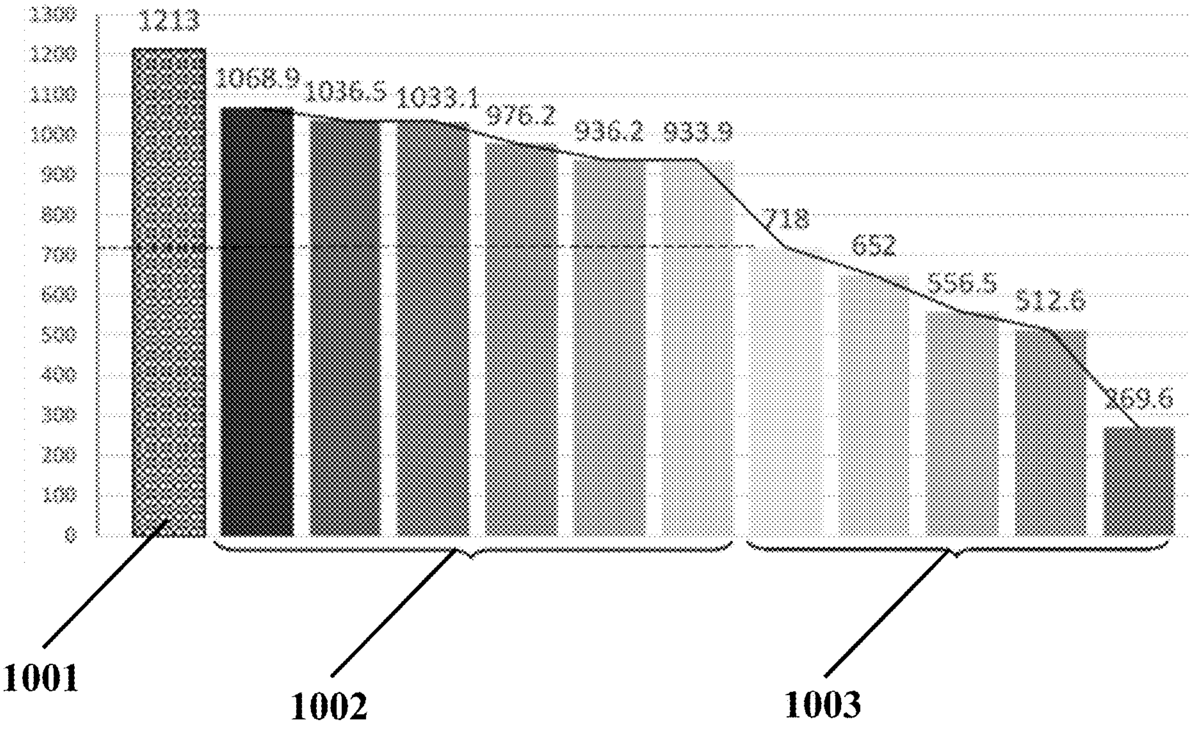

FIG. 10

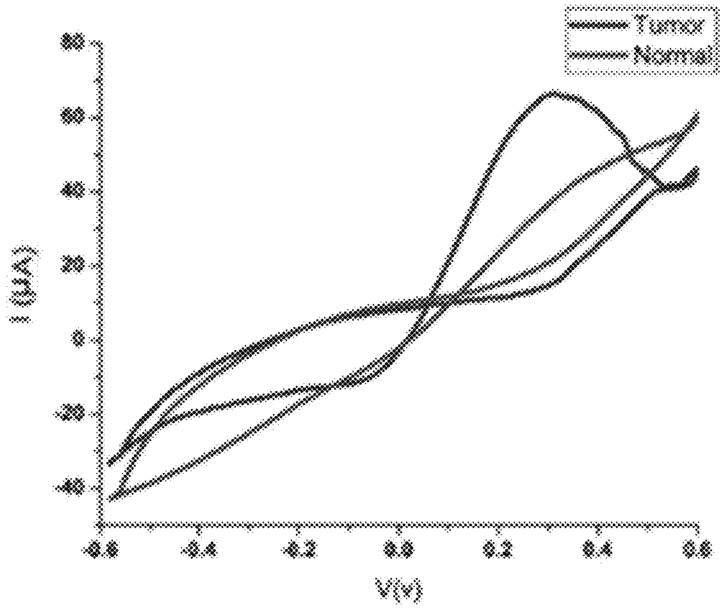

FIG. 11A

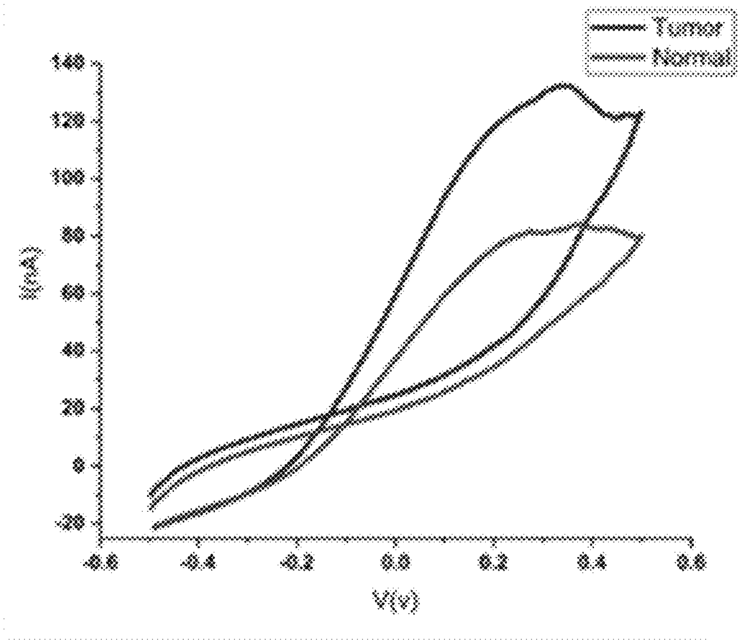

FIG. 11B

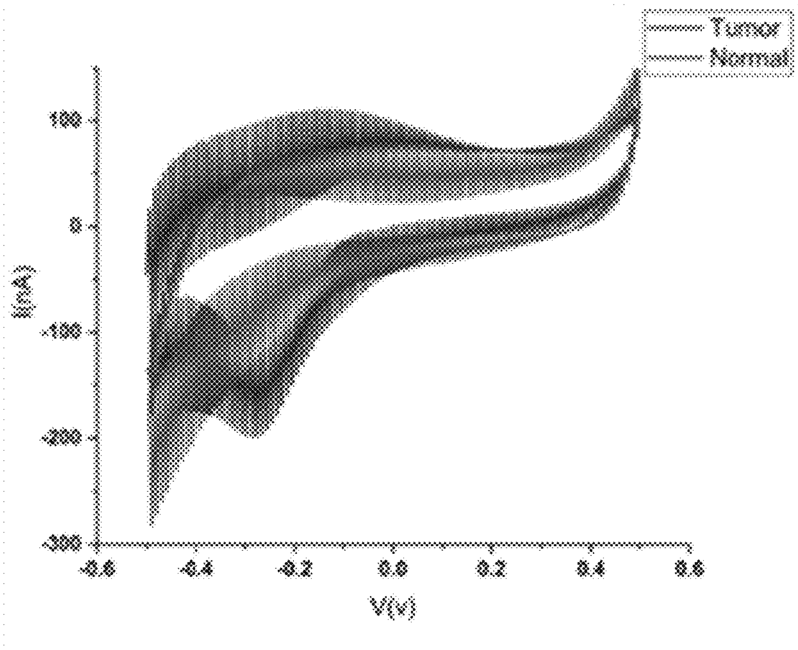

FIG. 11C

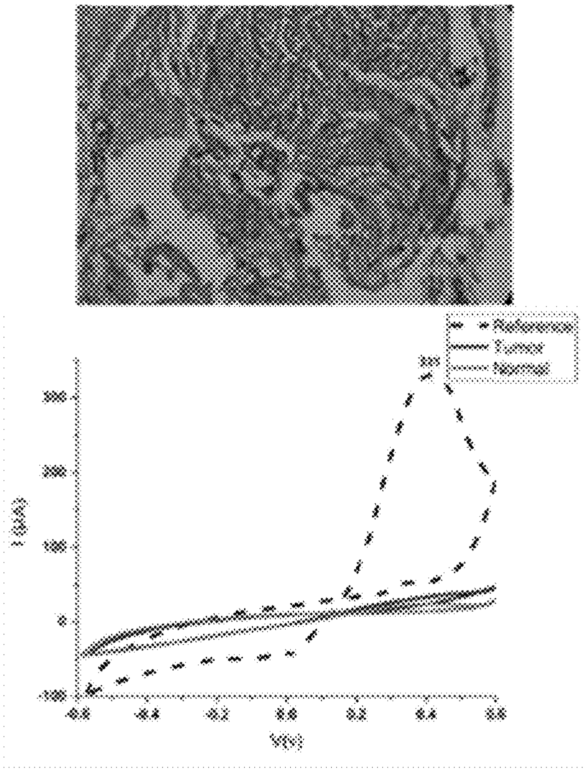
Reference
Tumor
Normal
I (μA)
300
200
100
0
-100
-0.6
-0.4
-0.2
0.0
0.2
0.4
0.6
V(v)

FIG. 12A

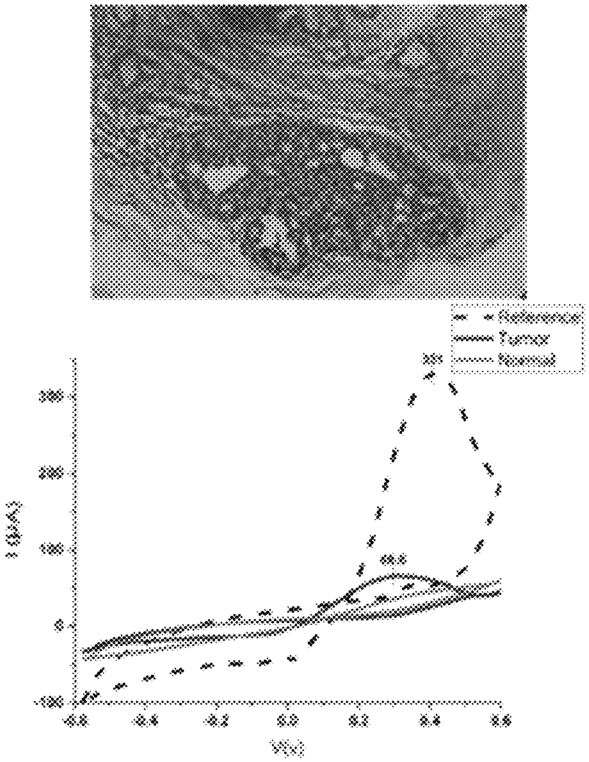
Reference
Tumor
Normal
300
200
100
0
-100
I (μA)
-0.6
-0.4
-0.2
0.0
0.2
0.4
0.6
V(v)

FIG. 12B

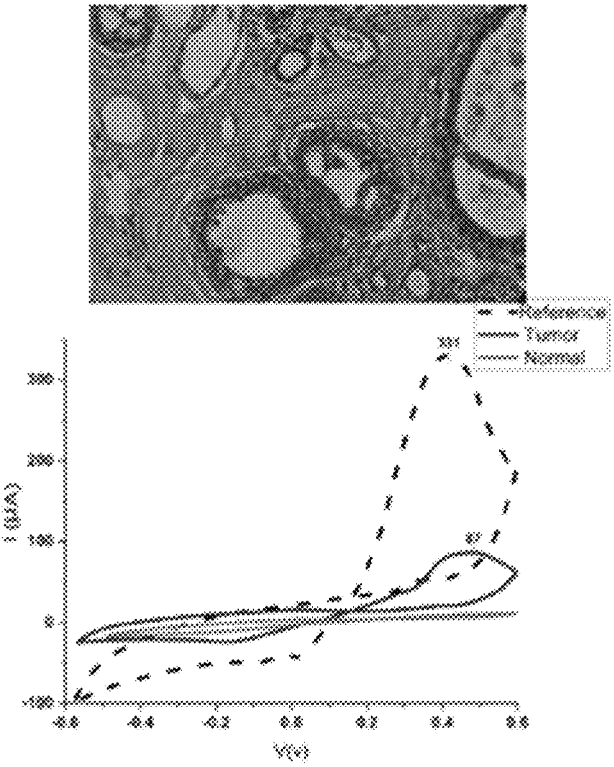
Reference
Tumor
Normal
331
87
300
200
100
0
-100
I (μA)
-0.6
-0.4
-0.2
0.0
0.2
0.4
0.6
V(v)

FIG. 12C

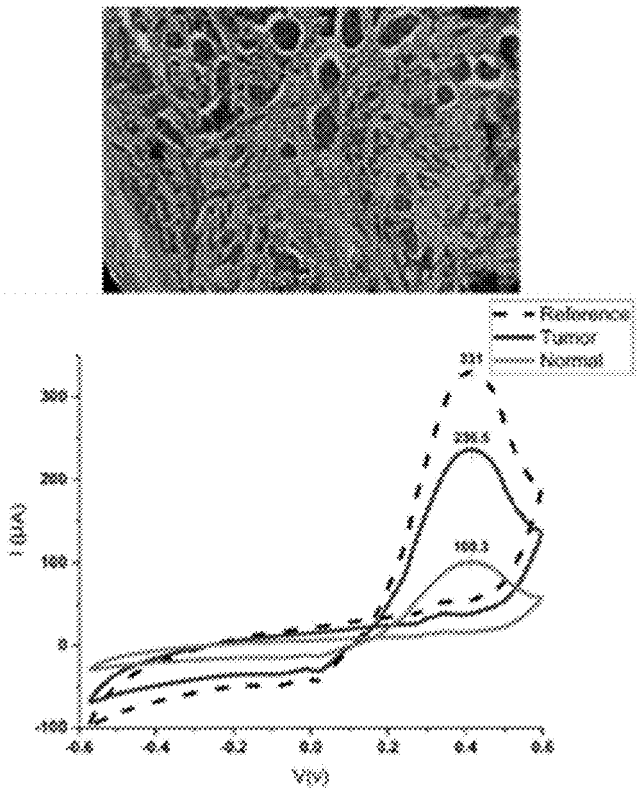
Reference
Tumor
Normal
331
236.5
100.3
300
200
100
0
-100
I (μA)
-0.6
-0.4
-0.2
0.0
0.2
0.4
0.6
V(v)

FIG. 12D

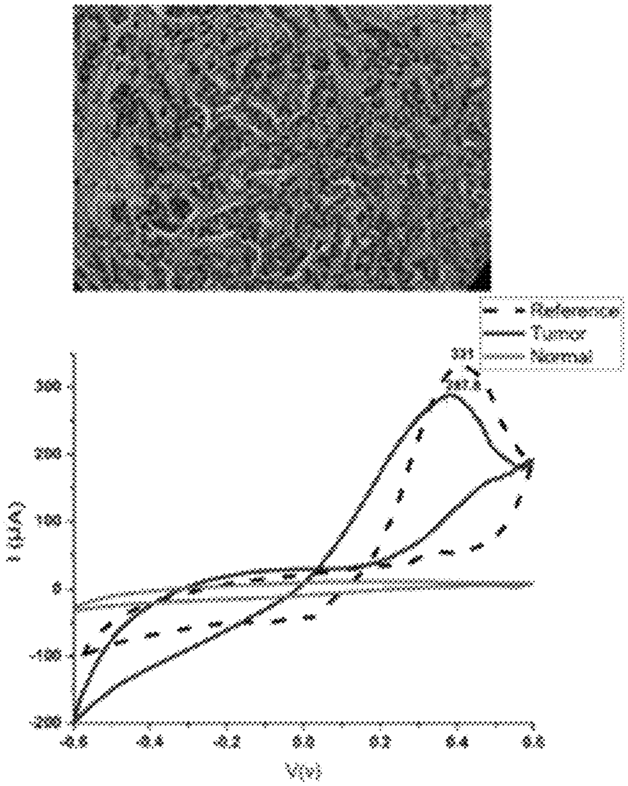
Reference
Tumor
Normal
331
287.9
300
200
100
0
-100
-200
I (µA)
-0.6
-0.4
-0.2
0.0
0.2
0.4
0.6
V(v)

FIG. 12E

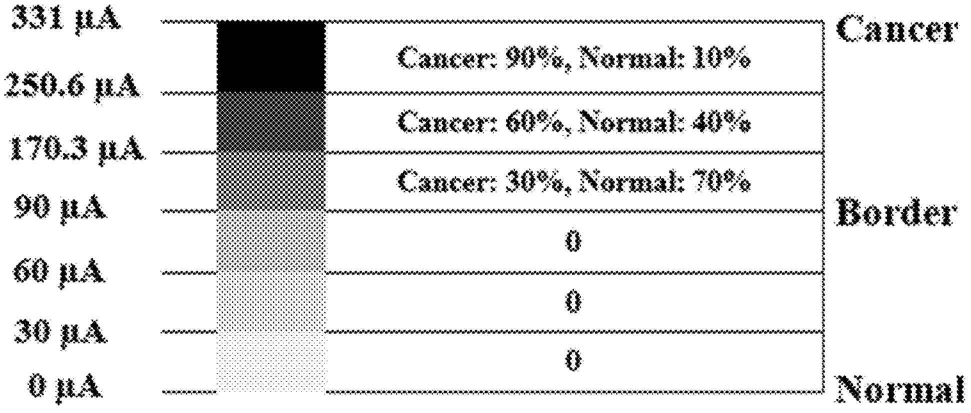

FIG. 13

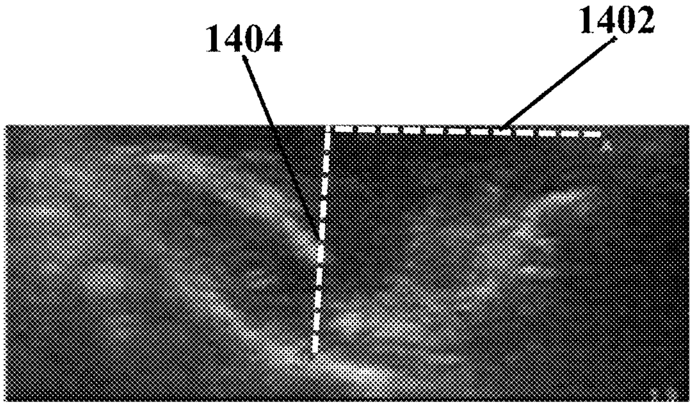

FIG. 14A

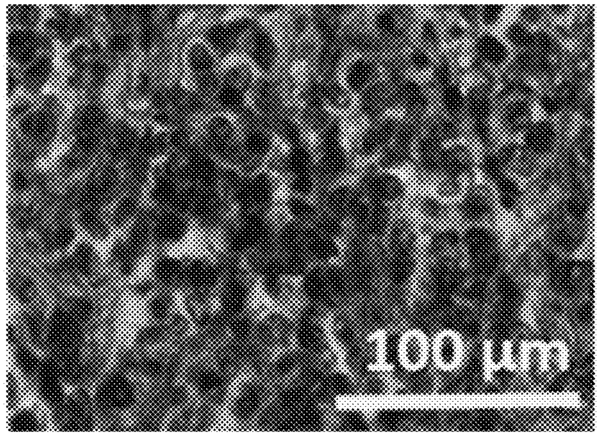

FIG. 14B

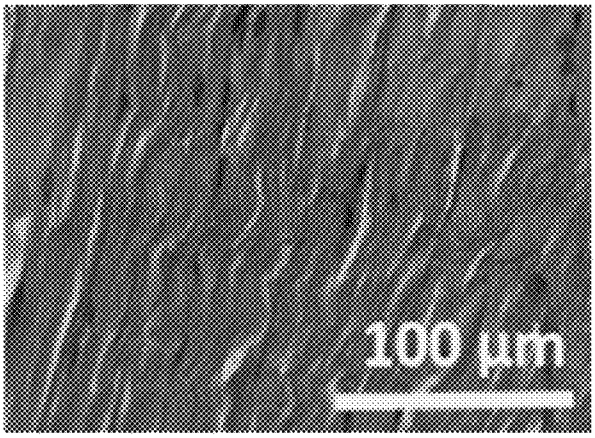

FIG. 14C

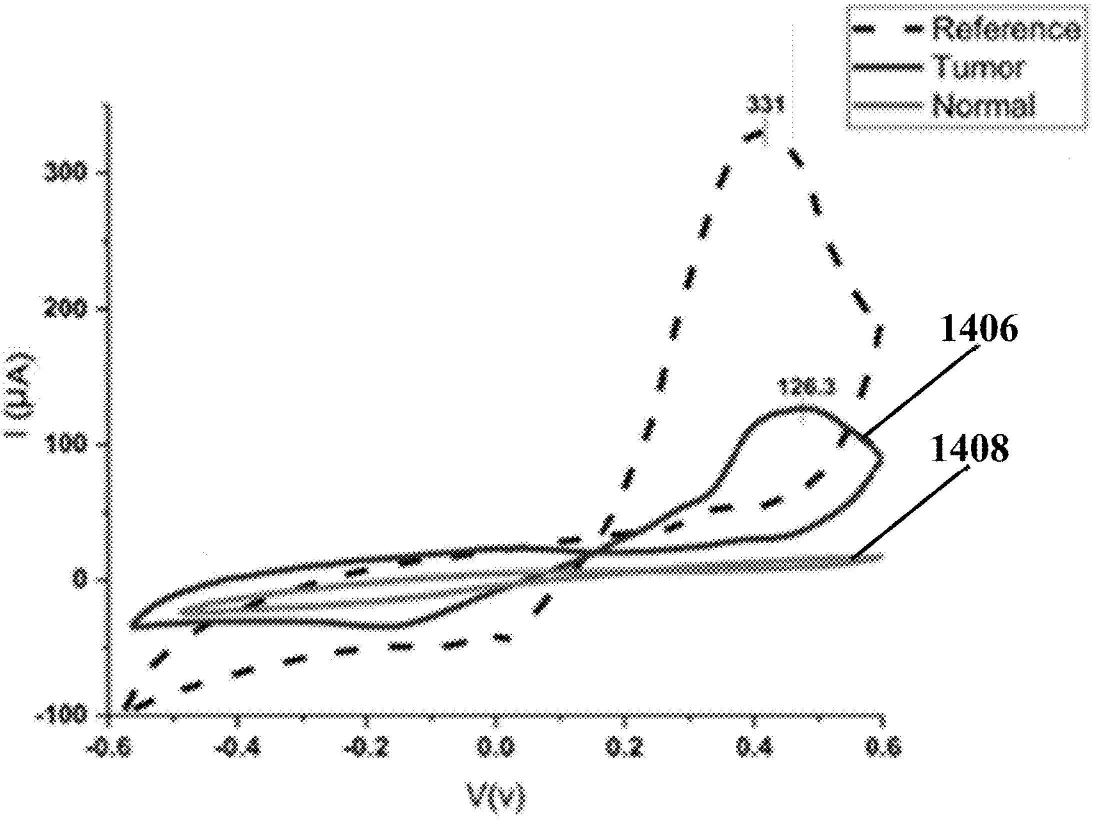

FIG. 14D

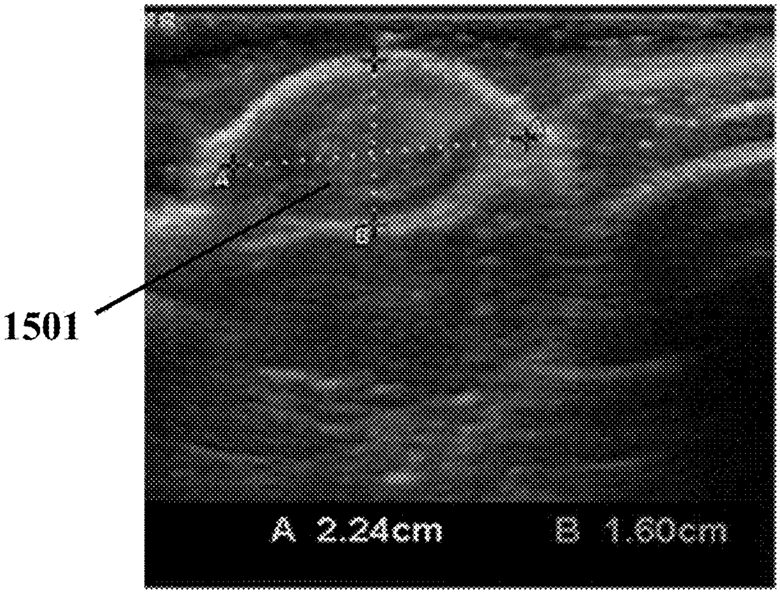

FIG. 15A

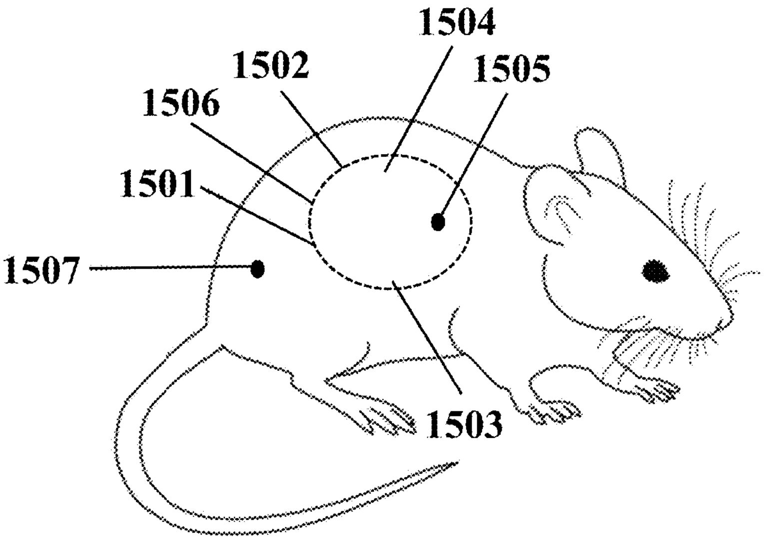

FIG. 15B

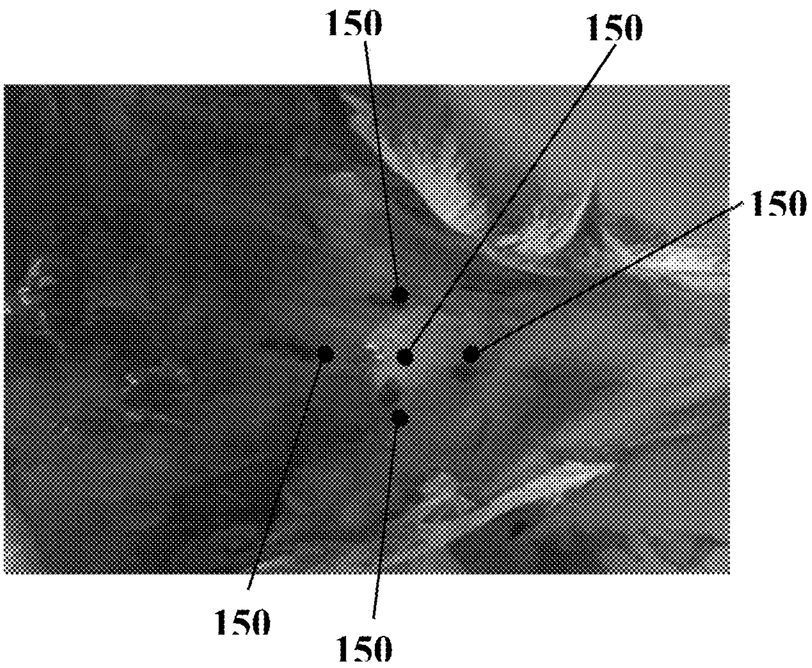

FIG. 15C

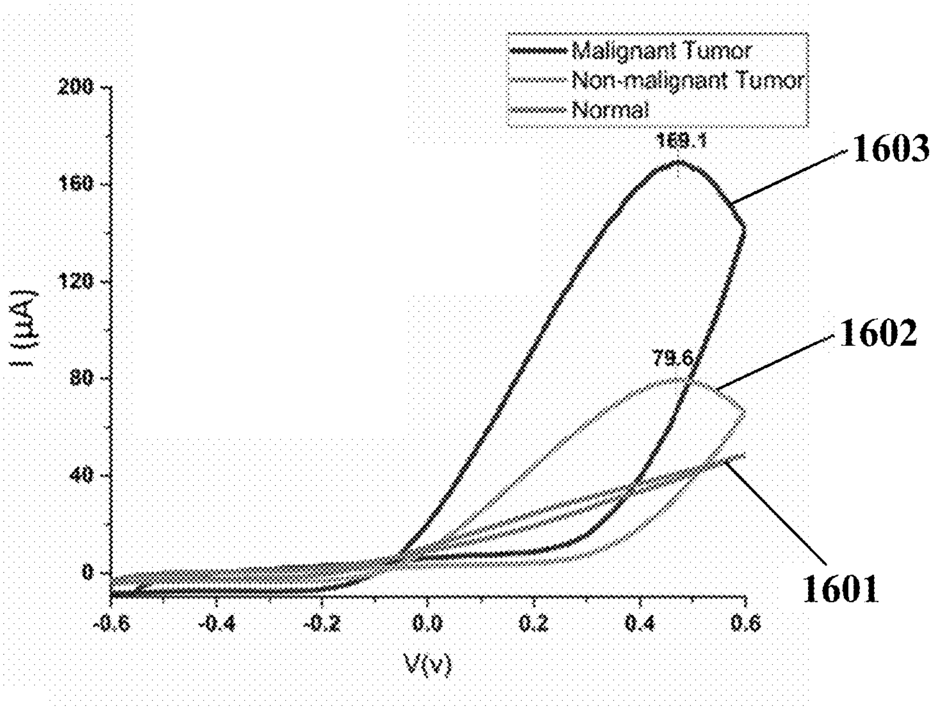

FIG. 16

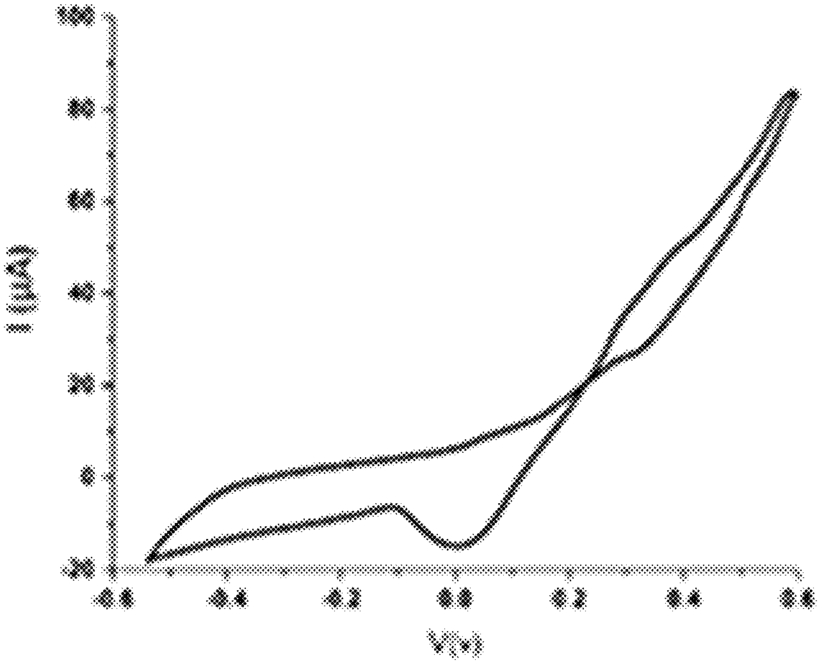

FIG. 17A

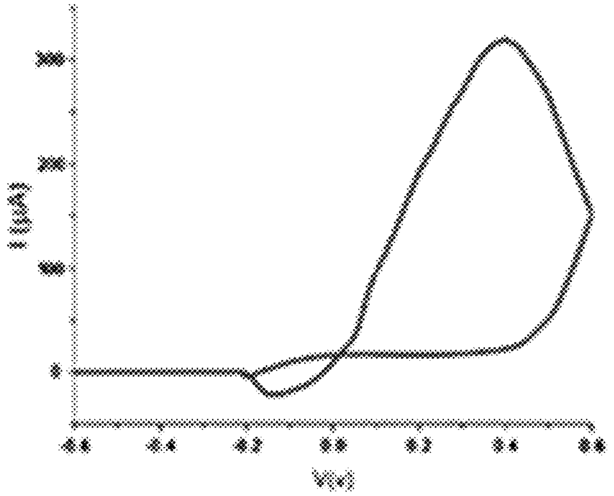

FIG. 17B

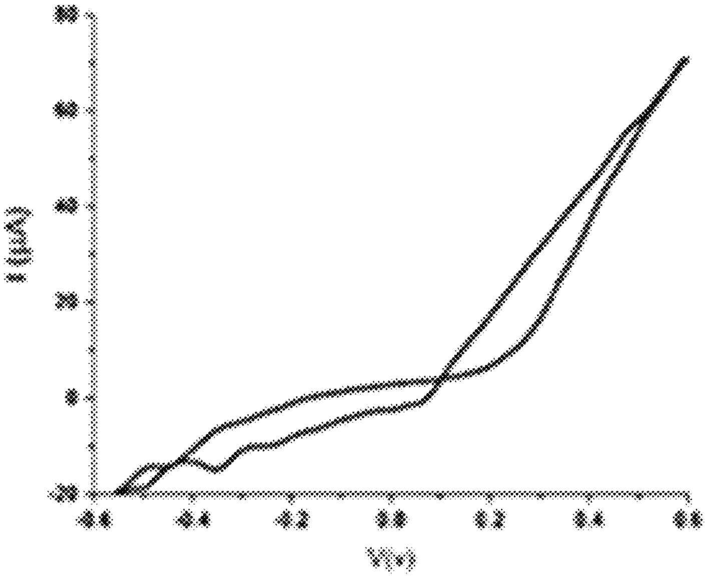

FIG. 17C

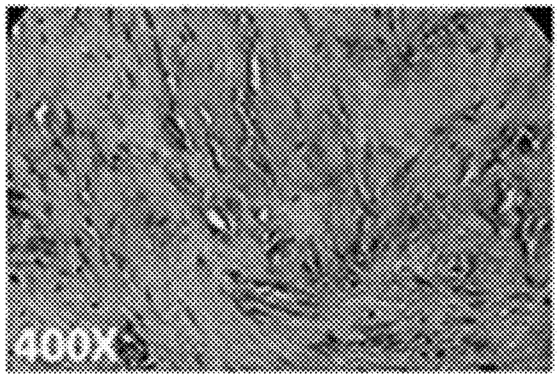

FIG. 17D

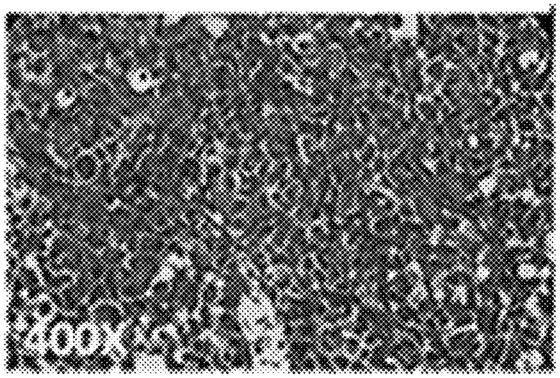

FIG. 17E

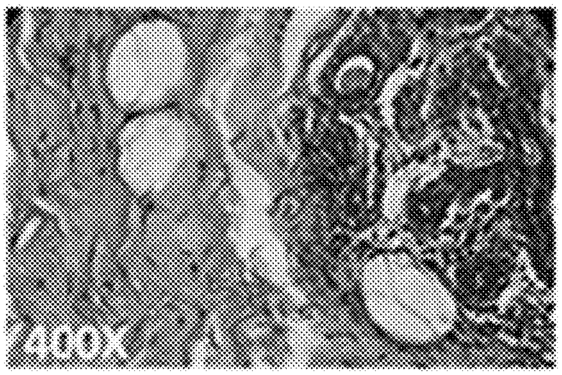

FIG. 17F

REAL-TIME AND LABEL FREE ANALYZER FOR IN-VITRO AND IN-VIVO DETECTING OF CANCER

CROSS-REFERENCE TO RELATED APPLICATION

This application claims the benefit of priority from U.S. Provisional Patent Application Ser. No. 62/522,115 filed on Jun. 20, 2017, and entitled "DIAGNOSIS OF CANCER TUMORS IN BIOPSY BREAST TISSUES" and U.S. Provisional Patent Application Ser. No. 62/563,673 filed on Sep. 27, 2017, and entitled "CANCER DIAGNOSTIC PROBE", which are both incorporated herein by reference in their entirety.

SPONSORSHIP STATEMENT

This application has been sponsored by Iran Patent Office, which does not have any rights in this application.

TECHNICAL FIELD

The present disclosure generally relates to cancer diagnosis, and particularly, to a system, sensor, and method for diagnosing cancerous regions before and during surgery via a real-time and label free approach.

BACKGROUND

Glycolysis is the intracellular biochemical conversion of one molecule of glucose into two molecules of pyruvate, which can be used to attain cellular energy. With the assistance of sufficient oxygen, pyruvate could be converted by pyruvate dehydrogenase (PDH) into acetylCoA which is crucial in a metabolizing process to produce ATP in an oxidative way. A physiological concentration of pyruvate in human normal epithelial tissue has been reported to 0.7 mmol/g. Also the lactate-to-pyruvate ratio (L/P ratio) as a reflection of cell's redox state, illustrates the balance between NAD+ and NADH+H+, depending on the interconversion of lactate and pyruvate via lactate dehydrogenase (LDH). The L/P ratio in normal epithelial tissues is less than 20:1. Markers and assays have been developed to trace the LADH, P, or L/P in the patients' specimen as diagnostic or prognostic factors which reveal the interests on lactate based cancer research. Moreover some methods have been developed to trace pyruvate by electrochemical methods with the assistance of chemically labelled working electrodes. However, there is still no substitutive label free methods and/or devices to replace expensive, complicated, and late-responsive clinical methods and devices such as pathology assays.

Hence, there is a need for cost-effective, label free and real-time methods and devices, especially sensors and method to use thereof to detect cancer in suspicious regions especially during cancer surgery like mastectomy to remove involved regions with precise margins to reduce resection of normal sites.

SUMMARY

This summary is intended to provide an overview of the subject matter of the present disclosure, and is not intended to identify essential elements or key elements of the subject matter, nor is it intended to be used to determine the scope of the claimed implementations. The proper scope of the present disclosure may be ascertained from the claims set forth below in view of the detailed description below and the drawings.

In one general aspect, the present disclosure describes an exemplary method for cancer diagnosis. The method may include putting an array of vertically aligned multi-walled carbon nanotubes (VAMWCNTs) of a sensor in contact with a suspicious sample, recording an electrochemical response from the suspicious sample, where the electrochemical response may include an oxidation current peak, and detecting a cancerous state in the suspicious sample responsive to a larger amount of the oxidation current peak than a threshold value. In an exemplary embodiment, the electrochemical response may include a cyclic voltammetry (CV) diagram of H_2O_2 related oxidation/reduction chemical reaction in biological cells within the suspicious sample. The concentration of H_2O_2 may be in correlation with the hypoxia glycolysis occurred in tumor cells. In an exemplary embodiment, the threshold value may include an oxidation current peak of about 80 μA or more.

In an exemplary implementation, detecting the cancerous state in the suspicious sample may include recording a reference electrochemical response from a reference solution, comparing the electrochemical response with the reference electrochemical response, and detecting a cancerous state in the suspicious sample responsive to a larger oxidation current peak of the electrochemical response in comparison with a reference oxidation current peak of the reference electrochemical response. In an exemplary embodiment, the reference solution may include a lactate solution with a lactate concentration of about 0.05 mM or more.

In an exemplary implementation, putting the array of VAMWCNTs of the sensor in contact with the suspicious sample may include one of dropping the suspicious sample onto the sensor, placing the suspicious sample onto the sensor, squeezing the sensor into the suspicious sample, inserting the sensor into the suspicious sample, and combinations thereof.

In an exemplary embodiment, the suspicious sample may include one of a liquid suspicious sample, a solid suspicious sample, and combinations thereof. In an exemplary embodiment, the suspicious sample may include one of a plurality of cell lines, a biopsied sample from a human or animal body, a removed sample from a human or animal body by surgery, a portion of a living tissue in a human or animal body, and a portion of a living tissue in a human or animal body during surgery.

In an exemplary implementation, the sensor may include a substrate, a catalyst layer, and three arrays of vertically aligned multi-walled carbon nanotubes (VAMWCNTs) grown on the catalyst layer. Three arrays of VAMWCNTs may include a working electrode that may include a first array of VAMWCNTs, a reference electrode that may include a second array of VAMWCNTs, and a counter electrode that may include a third array of VAMWCNTs. In an exemplary implementation, the sensor may further include a passivation layer between the substrate and the catalyst layer.

In an exemplary implementation, the sensor may include one of a CNT based electrochemical chip, and a cancer diagnosis probe (CDP). The substrate of the cancer diagnosis probe (CDP) may include three needles, where each needle of the three needles may be coated by an array of VAMWCNTs of the three arrays of VAMWCNTs.

In an exemplary implementation, recording the electrochemical response from the suspicious sample may include connecting the sensor to an electrochemical stimulator-analyzer, applying an electrical voltage on the sensor using the electrochemical stimulator-analyzer, and measuring the electrochemical response from the suspicious sample using the electrochemical stimulator-analyzer. In an exemplary embodiment, the electrochemical stimulator-analyzer may include a potentiostat.

In another aspect of the present disclosure, an electrochemical system for cancer diagnosis is disclosed. The electrochemical system may include a sensor, an electrochemical stimulator-analyzer, and an array of electrically conductive connectors. The sensor may include a working electrode, a reference electrode, and a counter electrode. Each of the working electrode, the reference electrode and the counter electrode may include an array of vertically aligned multi-walled carbon nanotubes (VAMWCNTs). The electrochemical stimulator-analyzer may be configured to measure electrochemical responses from the working electrode and the sensor may be connected to the electrochemical stimulator-analyzer via the array of electrically conductive connectors.

In an exemplary implementation, the sensor may include a CNT based electrochemical chip that may include a substrate, a passivation layer grown on the substrate, a catalyst layer coated on the passivation layer, and three arrays of VAMWCNTs grown on the catalyst layer.

In an exemplary implementation, the sensor may include a cancer diagnosis probe (CDP) that may include three needle electrodes, and a holding member. Each needle electrode of the three needles electrodes may include a tip. Each needle electrode may include a catalyst layer deposited on the tip of each needle electrode, and an array of VAMWCNTs grown on the tip of each needle electrode. The holding member may be configured to hold the three needle electrodes and three needle electrodes may be fixed on an end of the holding member.

In an exemplary implementation, each needle electrode of the three needle electrodes may include a steel needle with a diameter between about 100 μm and about 200 μm, and a length between about 0.1 cm and about 1 cm. Three needle electrodes may be fixed on the end of the holding member apart from each other with a distance (interspace) between about 1 mm and about 5 mm.

In an exemplary implementation, the electrochemical stimulator-analyzer system may include a potentiostat. The VAMWCNTs may include VAMWCNTs with a length of between about 0.5 μm and about 10 μm, and the VAMWCNTs may include VAMWCNTs with a diameter of between about 20 nm and about 100 nm.

BRIEF DESCRIPTION OF THE DRAWINGS

The drawing figures depict one or more implementations in accord with the present teachings, by way of example only, not by way of limitation. In the figures, like reference numerals refer to the same or similar elements.

FIG. **1**A illustrates a schematic view of an exemplary electrochemical system for cancer diagnosis, consistent with one or more exemplary embodiments of the present disclosure.

FIG. **1**B illustrates a schematic view of an exemplary CNT based electrochemical chip, consistent with one or more exemplary embodiments of the present disclosure.

FIG. **1**C illustrates a schematic view of an exemplary sensing well, consistent with one or more exemplary embodiments of the present disclosure.

FIG. **1**D illustrates a schematic view of an exemplary magnified portion of exemplary working electrode within exemplary sensing well of FIG. **1**C, consistent with one or more exemplary embodiments of the present disclosure.

FIG. **1**E illustrates a schematic view of an exemplary cancer diagnosis probe (CDP), consistent with one or more exemplary embodiments of the present disclosure.

FIG. **1**F illustrates a schematic view of an exemplary needle electrode of exemplary CDP corresponding to the working electrode, consistent with one or more exemplary embodiments of the present disclosure.

FIG. **1**G illustrates a schematic view of an exemplary magnified portion of a tip of exemplary needle electrode of FIG. **1**C, consistent with one or more exemplary embodiments of the present disclosure.

FIG. **2**A illustrates an exemplary implementation of a method for cancer diagnosis, consistent with one or more exemplary embodiments of the present disclosure.

FIG. **2**B illustrates a schematic implementation of putting the array of vertically aligned multi-walled carbon nanotubes (VAMWCNTs) grown on tip of each needle electrode of three needles electrodes of exemplary CDP in contact with exemplary suspicious sample, consistent with one or more exemplary embodiments of the present disclosure.

FIG. **2**C illustrates an implementation of detecting the cancerous state in the suspicious sample, consistent with one or more exemplary embodiments of the present disclosure.

FIG. **3**A illustrates a schematic view of exemplary electrochemical reactions involved on sensor including exemplary VAMWCNTs as shown in FIGS. **1**D and **1**G, consistent with one or more exemplary embodiments of the present disclosure.

FIG. **3**B illustrates a schematic overview of mitochondrial electron and proton fluxes in hypoxia, consistent with one or more exemplary embodiments of the present disclosure.

FIG. **4** illustrates a field emission scanning electron microscopy (FESEM) image of the VAMWCNTs array on a portion of an exemplary fabricated CNT based electrochemical chip, consistent with one or more exemplary embodiments of the present disclosure.

FIG. **5**A illustrates a FESEM image of a tip of a needle electrode of an exemplary fabricated cancer diagnostic probe (CDP) coated with an array of VAMWCNTs on the tip, consistent with one or more exemplary embodiments of the present disclosure.

FIG. **5**B illustrates a FESEM image of a first portion of an exemplary VAMWCNTs array grown on the tip of the needle electrode of exemplary fabricated CDP, consistent with one or more exemplary embodiments of the present disclosure.

FIG. **5**C illustrates a FESEM image of a second portion of an exemplary VAMWCNTs array grown on the tip of the needle electrode of exemplary fabricated CDP, consistent with one or more exemplary embodiments of the present disclosure.

FIG. **5**D illustrates a FESEM image of a third portion of an exemplary VAMWCNTs array grown on the tip of the needle electrode of exemplary fabricated CDP, consistent with one or more exemplary embodiments of the present disclosure.

FIG. **6**A illustrates the CV diagrams of L-lactic acid solution individually recorded by electrochemical sensors fabricated from platinum (Pt), Gold (Au), amorphous glassy carbon (GC) and carbon nanotube (CNT) working electrodes (WEs), consistent with one or more exemplary embodiments of the present disclosure.

FIG. **6**B illustrates the CV diagrams of solutions with various concentrations of Hydrogen Peroxide (H_2O_2) resulted from the lactate turn to H_2O_2 and pyruvate recorded by electrochemical sensors with CNT arrays working electrode, consistent with one or more exemplary embodiments of the present disclosure.

FIG. **6**C illustrates the CV diagrams of H_2O_2 contained lactate solution in comparison with two cell culture solutions recorded by electrochemical sensors with CNT arrays working electrode, consistent with one or more exemplary embodiments of the present disclosure.

FIG. **7** illustrates the CV diagrams of hypoxic glycolysis in MCF 10A, MCF-7, MDA-MB-231, and MDA-MB-468 cell lines in comparison with H_2O_2 contained lactate solution and RPMI measured and recorded by exemplary CNT based electrochemical chip, consistent with one or more exemplary embodiments of the present disclosure.

FIG. **8**A illustrates the CV responses of the solution media of different normal and cancerous cell lines in various phenotypes for Colon (COR-L 105, SW-480, HT-29) cell lines in comparison with Reference diagram for solution H_2O_2 contained solution with a lactate concentration of about 0.3 mM, consistent with one or more exemplary embodiments of the present disclosure.

FIG. **8**B illustrates the CV responses of the solution media of different normal and cancerous cell lines in various phenotypes for Hematopoietic (1301, LCL-PI 1) cell lines in comparison with Reference diagram for H_2O_2 contained solution with a lactate concentration of about 0.3 mM, consistent with one or more exemplary embodiments of the present disclosure.

FIG. **8**C illustrates the CV responses of the solution media of different normal and cancerous cell lines in various phenotypes for Liver (HEP G2) cell lines in comparison with Reference diagram for H_2O_2 contained lactate solution with a lactate concentration of about 0.3 mM, consistent with one or more exemplary embodiments of the present disclosure.

FIG. **8**D illustrates the CV responses of the solution media of different normal and cancerous cell lines in various phenotypes for Lung (QU-DB, MRC-5) cell lines in comparison with Reference diagram for H_2O_2 contained lactate solution with a lactate concentration of about 0.3 mM, consistent with one or more exemplary embodiments of the present disclosure.

FIG. **8**E illustrates the CV responses of the solution media of different normal and cancerous cell lines in various phenotypes for Mouth (KB) cell lines in comparison with Reference diagram for H_2O_2 contained lactate solution with a lactate concentration of about 0.3 mM, consistent with one or more exemplary embodiments of the present disclosure.

FIG. **8**F illustrates the CV responses of the solution media of different normal and cancerous cell lines in various phenotypes for Neuron (BE(2)-C, LAN-5) cell lines in comparison with Reference diagram for H_2O_2 contained lactate solution with a lactate concentration of about 0.3 mM, consistent with one or more exemplary embodiments of the present disclosure.

FIG. **8**G illustrates the CV responses of the solution media of different normal and cancerous cell lines in various phenotypes for Prostate (PC-3, Du-145) cell lines in comparison with Reference diagram for H_2O_2 contained lactate solution with a lactate concentration of about 0.3 mM, consistent with one or more exemplary embodiments of the present disclosure.

FIGS. **9**A-**9**F illustrate the cytopathological results (top side) and electrochemical responses (bottom side) of the breast tissues removed by biopsy or surgery from 6 suspicious patients to cancer, consistent with one or more exemplary embodiments of the present disclosure.

FIG. **10** illustrates a columnar diagram of electrochemical responses of the breast tissues removed by biopsy or surgery from 11 suspicious patients to cancer, consistent with one or more exemplary embodiments of the present disclosure.

FIG. **11**A illustrates CV response of exemplary CDP with all three needles covered by VAMWCNTs immediately after connection to the tissues, consistent with one or more exemplary embodiments of the present disclosure.

FIG. **11**B illustrates CV response of exemplary CDP with only working electrode covered by VAMWCNTs immediately after connection to the tissues, consistent with one or more exemplary embodiments of the present disclosure.

FIG. **11**C illustrates CV response of exemplary CDP with non-CNT covered by needles immediately after connection to the tissues, consistent with one or more exemplary embodiments of the present disclosure.

FIGS. **12**A-**12**E illustrate CV responses recorded by exemplary CDP (needle based electrochemical sensor) from the resected tissues from five patients among 50 individual patients suspicious to breast cancer (bottom side) in comparison with images obtained by conventional pathological methods (H&E) (top side), consistent with one or more exemplary embodiments of the present disclosure.

FIG. **13** illustrates a summary of categorized regimes of CV responses recorded by exemplary CDP from the resected tissues from five patients among 50 individual patients suspicious to breast cancer representing CV regimes along a spectrum from a completely non-cancerous state to cancerous state, consistent with one or more exemplary embodiments of the present disclosure.

FIG. **14**A illustrates a sonography image from a tumor side taken from an exemplary mouse tumorized by 4T1 breast cancer cell lines, consistent with one or more exemplary embodiments of the present disclosure.

FIG. **14**B illustrates H&E image from the tumor side taken from exemplary tumorized mouse by 4T1 breast cancer cell lines, consistent with one or more exemplary embodiments of the present disclosure.

FIG. **14**C illustrates H&E image from a normal/healthy side taken from exemplary tumorized mouse by 4T1 breast cancer cell lines, consistent with one or more exemplary embodiments of the present disclosure.

FIG. **14**D illustrates CV diagrams of normal and tumor regions/sides of exemplary tumorized mouse by 4T1 breast cancer cell lines calibrated by a Reference CV diagram from H_2O_2 contained lactate solution with a lactate concentration of about 0.3 mM obtained using exemplary CDP, consistent with one or more exemplary embodiments of the present disclosure.

FIG. **15**A illustrates a sonography image from a tumor taken from an exemplary mouse tumorized by 4T1 breast cancer cell lines, consistent with one or more exemplary embodiments of the present disclosure.

FIG. **15**B illustrates exemplary six analyzed regions of an exemplary tumorized mouse among the exemplary five tumorized mice before surgery, consistent with one or more exemplary embodiments of the present disclosure.

FIG. **15**C illustrates exemplary six analyzed regions of an exemplary tumorized mouse among the exemplary five tumorized mice during surgery, consistent with one or more exemplary embodiments of the present disclosure.

FIG. **16** illustrates comparative diagram of CDP responses in interaction with normal, nonmalignant tumor, and malignant tumor recorded from individual mice, consistent with one or more exemplary embodiments of the present disclosure.

FIG. **17**A illustrates CV response diagram obtained by applying exemplary CDP in detection of suspicious margins during breast cancer surgery for a known normal region, consistent with one or more exemplary embodiments of the present disclosure.

FIG. **17**B illustrates CV response diagram obtained by applying exemplary CDP in detection of suspicious margins during breast cancer surgery for a suspicious region, consistent with one or more exemplary embodiments of the present disclosure.

FIG. **17**C illustrates CV response diagram obtained by applying exemplary CDP in detection of suspicious margins during breast cancer surgery for another suspicious region, consistent with one or more exemplary embodiments of the present disclosure.

FIG. **17**D illustrates an H&E resulted image after the surgery for a known normal region, consistent with one or more exemplary embodiments of the present disclosure.

FIG. **17**E illustrates an H&E resulted image after the surgery for a suspicious region, consistent with one or more exemplary embodiments of the present disclosure.

FIG. **17**F illustrates an H&E resulted image after the surgery for another suspicious region, consistent with one or more exemplary embodiments of the present disclosure.

DETAILED DESCRIPTION

In the following detailed description, numerous specific details are set forth by way of examples in order to provide a thorough understanding of the relevant teachings. However, it should be apparent that the present teachings may be practiced without such details. In other instances, well known methods, procedures, components, and/or circuitry have been described at a relatively high-level, without detail, in order to avoid unnecessarily obscuring aspects of the present teachings. The following detailed description is presented to enable a person skilled in the art to make and use the methods and devices disclosed in exemplary embodiments of the present disclosure. For purposes of explanation, specific nomenclature is set forth to provide a thorough understanding of the present disclosure. However, it will be apparent to one skilled in the art that these specific details are not required to practice the disclosed exemplary embodiments. Descriptions of specific exemplary embodiments are provided only as representative examples. Various modifications to the exemplary implementations will be readily apparent to one skilled in the art, and the general principles defined herein may be applied to other implementations and applications without departing from the scope of the present disclosure. The present disclosure is not intended to be limited to the implementations shown, but is to be accorded the widest possible scope consistent with the principles and features disclosed herein.

A number of current methods utilize lactate and/or pyruvate as cancer markers. However, herein the oxidation of Hydrogen Peroxide (H_2O_2) molecules measured by carbon nanotubes (CNTs) based electrodes is utilized to detect cancer and especially distinguish cancerous regions from healthy regions in a suspicious tissue. The main consequence of pyruvate formation from lactate is release of H_2O_2 molecules as the main byproduct of hypoxia glycolysis. An abnormal redox state appears in cancer cells based on modulation of hypoxia with increased pyruvate concentration and lactate-to-pyruvate ratio (L/P ratio) which results in increasing the concentration of H_2O_2 in interstitial fluid (stroma). So, determination of H_2O_2 molecules would be an indication for the presence of cancer cells in a tissue. As H_2O_2 is an active and non-stable molecule it would turn to O_2, H^+ and release electrons which are great target charges for electrochemical sensation.

Herein, an electrochemical approach based on multi-walled carbon nanotubes (MWCNTs) electrodes is disclosed for fast tracking of hypoxia glycolysis in the interstitial fluid of biopsied tissues suspicious to cancer, such as breast tissues. Electrochemical reduction of H_2O_2 molecules, produced in lactate to pyruvate transformation, on the electrodes of disclosed system may present a significant quantitate response signal in correlation with the presence of cancer cells in a suspicious sample. Here, a cancer diagnostic probe (CDP) based on vertically aligned multi-walled carbon nanotubes (VAMWCNTs) arrays as sensing electrode with direct and selective electron transfer abilities in interaction with H_2O_2 may be utilized.

Disclosed herein may include a label free method for diagnosis of the presence of cancer in suspicious regions based on determination of the hypoxia glycolysis in a quantitative manner. The method may be based on measuring the oxidative currents released during glycolysis from the tissue. A matched diagram between an electrochemical response measured from a suspicious sample and cancerous state curves may be utilized for a final diagnostic result. Over expression of glycolysis assisted mRNAs in cancerous samples may be observed as an indicator of a presence of cancer in a sample. Exemplary method may be applied as an alternative for frozen pathology during the surgery with faster and more precise efficiency. Furthermore, a label free system including an electrochemical sensor with integrated three CNT based electrodes is disclosed for tracking hypoxia glycolysis via detecting electrochemical reduction of H_2O_2 molecules, which may be produced in Lactate to pyruvate transformation in cancer cells. Exemplary simple and label free electrochemical assay may also be used for measuring the drug resistance of the tumors as a pre therapeutic prediction (as a new prognostic factor) to increase the survival rate in future.

In some implementations, exemplary electrochemical sensor may include an integrated sensor on the needles, named herein as a cancer diagnostic probe (CDP). Exemplary CDP may be fabricated and utilized in real-time on the suspicious regions to cancer before and during surgery in patients (In vivo). The domain of suspicious regions with a resolution of about 3 mm may be detected using exemplary method and CDP. The significant specification of CDP rather than recently reported real-time diagnostic methods, such as mass-spec, may allow the CDP to track the cancer involved regions before surgery by squeezing exemplary CDP to suspicious regions through the skin with the tracking resolution of 3 mm. In conventional diagnostic protocols, to precisely remove the cancer regions during surgery, a frozen sample from each suspicious region may need to be sent for pathologists. The pathology results may be available after about 15 minutes with the false negative response ratio of about 10%. Whereas, a cancer region may be distinguished in-situ utilizing exemplary CDP in less than about 10 seconds or even instantaneously before or during surgery and without any need for resecting and freezing a sample from a patient. The diagnostic information obtained by exemplary CDP may be used to detect cancer in marginally suspicious regions with rare distributions of cancer cells filtrated between normal stroma in less than about 20 seconds during the surgery or biopsy of live animal or human models without any requirement of tissue resection and preparation for frozen pathology. Exemplary CDP may be also utilized to detect an accurate location of cancer involved regions before surgery in superficial tumors.

Moreover, exemplary sensor may include a CNT based electrochemical chip for in vitro cancer diagnosis in suspicious samples. Exemplary CNT based electrochemical chip may include an array of electrodes of VAMWCNTs used in electrochemical assays. Both liquid and solid suspicious samples may be analyzed using exemplary CNT based electrochemical chip to detect a cancer presence within the suspicious samples.

FIG. **1**A shows a schematic view of an electrochemical system **100** for cancer diagnosis, consistent with one or more exemplary embodiments of the present disclosure. Exemplary electrochemical system **100** may include an exemplary sensor **102**, an electrochemical stimulator-analyzer **104**, and an array of electrically conductive connectors **106**. Exemplary sensor **102** may be put in contact with a suspicious sample for cancer. Exemplary sensor **102** may include an integrated three-electrodes array, which may include the working electrode **108**, the counter electrode **110**, and the reference electrode **112**. Each of the working electrode **108**, the counter electrode **110** and the reference electrode **112** may include an array of vertically aligned multi-walled carbon nanotubes (VAMWCNTs). The electrochemical stimulator-analyzer **104** may be configured to measure electrochemical responses from the working electrode **108** and sensor **102** may be connected to the electrochemical stimulator-analyzer **104** via the array of electrically conductive connectors **106**.

In an exemplary implementation, exemplary electrochemical system **100** may be configured to detect a cancerous state via measuring H_2O_2 during hypoxia glycolysis in the suspicious sample for cancer. Exemplary electrochemical system **100** may be utilized by an exemplary method for cancer diagnosis described herein below.

In an exemplary embodiment, electrochemical stimulator-analyzer **104** may include a device that may be capable of measuring cyclic voltammetry (CV) based diagrams. In an exemplary embodiment, electrochemical stimulator-analyzer **104** may include a potentiostat.

In an exemplary implementation, electrochemical system **100** may further include a processor **114** that may be utilized for recording and analyzing electrochemical measurements that may be measured by electrochemical stimulator-analyzer **104**. Processor **114** may also be used for controlling electrochemical stimulations that may be carried out by electrochemical stimulator-analyzer **104**. In an exemplary embodiment, processor **114** may include an EVIUM readout system.

In an exemplary implementation, sensor **102** may include a CNT based electrochemical chip that may be configured to conduct in vitro cancer diagnosis assays. FIG. **1**B shows a schematic view of exemplary CNT based electrochemical chip **102**, consistent with one or more exemplary embodiments of the present disclosure. Exemplary CNT based electrochemical chip **102** may include at least one sensing well **120** and one array of electrically conductive connectors **106**. FIG. **1**C shows a schematic view of exemplary sensing well **120**, consistent with one or more exemplary embodiments of the present disclosure. Each sensing well **120** may include a substrate **122**, a passivation layer **124** that may be grown on substrate **122**, a catalyst layer **126** that may be coated or deposited and subsequently patterned on the passivation layer **124**, and three arrays of VAMWCNTs that may be grown on the catalyst layer **126**. Three arrays of VAMWCNTs may include the working electrode **108**, the counter electrode **110**, and the reference electrode **112**.

In an exemplary embodiment, substrate **122** may include a silicon chip or wafer. Passivation layer **124** may include a layer of SiO_2 with a thickness of less than about 500 nm that may be grown by wet oxidation furnace on the surface of on substrate **122**. Catalyst layer **126** may include a layer of Nickel (Ni) with a thickness of less than about 10 nm that may be coated on passivation layer **124** by an E-beam evaporation system at a temperature of about 120° C. with depositing rate of about 0.1 Angstroms/s. Three arrays of VAMWCNTs (the working electrode **108**, the counter electrode **110**, and the reference electrode **112**) may be grown on catalyst layer **126** using a direct current plasma enhanced chemical vapor deposition (DC-PECVD) system. The growth process of VAMWCNTs may include three steps of firstly, annealing at a temperature of about 680° C. in an H_2 environment with a flow rate of about 35 standard cubic centimeters per minute (sccm) for about 30 minutes; secondly, graining, including plasma hydrogenation of surface for about 5 minutes with the intensity of about 5.5 $W \cdot cm^{-2}$ that may result in the catalyst layer **126** graining and formation of Ni nano-sized islands, and finally, growth of VAMWCNTs by introducing a plasma of C_2H_2 and H_2 mixture with flow rates of about 5 sccm and about 35 sccm to the chamber for about 15 minutes. Each of the VAMWCNTs may have a length between about 0.5 μm and about 5 μm and a diameter between about 20 nm and about 100 nm. The working electrode **108** may be grown on an area of about 1 cm×1 cm, the counter electrode **110** may be grown on an area of about 1 cm×1 cm, and the reference electrode **112** may be grown on an area of about 0.5 cm×0.5 cm.

FIG. **1**D shows a schematic view of an exemplary magnified portion **128** of exemplary working electrode **108** within exemplary sensing well **120** of FIG. **1**C, consistent with one or more exemplary embodiments of the present disclosure. Exemplary VAMWCNTs **130** of an array of VAMWCNTs of working electrode **108** may be grown vertically on catalyst layer **126**. Catalyst layer **126** may be coated or deposited and subsequently patterned on the passivation layer **124**, where passivation layer **124** may be grown on substrate **122**.

In an exemplary implementation, sensor **102** may include a cancer diagnosis probe (CDP) that may be configured to conduct in vivo cancer diagnosis assays. FIG. **1**E shows a schematic view of exemplary cancer diagnosis probe (CDP) **102**, consistent with one or more exemplary embodiments of the present disclosure. Exemplary cancer diagnosis probe (CDP) may include three needle electrodes **132**, **134**, and **136** as exemplary implementations of the working electrode **108**, the counter electrode **110**, and the reference electrode **112**, respectively. Moreover, CDP **102** may include a holding member **138** that may be configured to hold three needle electrodes **132**, **134**, and **136**. Three needle electrodes **132**, **134**, and **136** may be fixed on one end **140** of the holding member **138**.

FIG. **1**F shows a schematic view of an exemplary needle electrode **132** corresponding to the working electrode **108**, consistent with one or more exemplary embodiments of the present disclosure. Referring to FIG. **1**F, each needle electrode of three needles electrodes **132**, **134**, and **138** may include a tip **142**. Each needle electrode of the three needles electrodes **132**, **134**, and **136** may include a catalyst layer **144** that may be deposited on tips **142** of three needles electrodes **132**, **134**, and **136** and an array of VAMWCNTs

146 that may be grown on catalyst layer **144** on tip **142** of each needle electrode of three needles electrodes **132**, **134**, and **138**.

In an exemplary embodiment, each needle electrode of three needles electrodes **132**, **134**, and **138** may include a steel needle with a diameter between about 100 μm and about 200 μm, and a length between about 0.1 cm and about 1 cm. Three needle electrodes **132**, **134**, and **138** may be fixed on the end **140** of the holding member **138** apart from each other with a distance (interspace) between each other in a range of about 1 mm to about 5 mm.

In an exemplary embodiment, catalyst layer **144** may include a layer of Nickel (Ni) with a thickness of less than about 10 nm that may be coated on tip **142** of each needle electrode by an E-beam evaporation system at a temperature of about 120° C. with a depositing rate of about 0.1 Angstroms/s. Three arrays of VAMWCNTs (the working electrode **108**, the counter electrode **110**, and the reference electrode **112**) may be grown on catalyst layer **144** using a direct current plasma enhanced chemical vapor deposition (DC-PECVD) system as described herein above.

FIG. **1**G shows a schematic view of an exemplary magnified portion **148** of tip **142** of exemplary needle electrode **132** shown in FIG. **1**F, consistent with one or more exemplary embodiments of the present disclosure. Exemplary VAMWCNTs **130** of an array of VAMWCNTs **146** may be grown vertically on catalyst layer **144**. Catalyst layer **144** may be coated or deposited on a surface of tip **142**.

In another aspect of the present disclosure, a method for cancer diagnosis is disclosed. FIG. **2**A shows an exemplary implementation of method **200** for cancer diagnosis, consistent with one or more exemplary embodiments of the present disclosure. Method **200** may include putting an array of vertically aligned multi-walled carbon nanotubes (VAMWCNTs) of a sensor in contact with a suspicious sample (step **202**), recording an electrochemical response from the suspicious sample, where the electrochemical response may include an oxidation current peak (step **204**), and detecting a cancerous state in the suspicious sample responsive to a larger amount of the oxidation current peak than a threshold value (step **206**). The sensor may be similar to exemplary sensor **102** described hereinabove.

Step **202** may include putting the array of vertically aligned multi-walled carbon nanotubes (VAMWCNTs) of the sensor in contact with the suspicious sample. In an exemplary implementation, putting the array of VAMWCNTs of the sensor in contact with the suspicious sample may include one of dropping the suspicious sample onto the sensor, placing the suspicious sample onto the sensor, squeezing the sensor into the suspicious sample, inserting the sensor into the suspicious sample, and combinations thereof.

In an exemplary embodiment, the suspicious sample may include one of a liquid suspicious sample, a solid suspicious sample, and combinations thereof. In an exemplary embodiment, the suspicious sample may include one of a plurality of cell lines, a biopsied sample from a human or animal body, a removed sample from a human or animal body by surgery, a portion of a living tissue in a human or animal body, and a portion of a living tissue in a human or animal body during surgery.

In an exemplary implementation, the sensor may be similar to sensor **102** and may include a substrate, a catalyst layer, and three arrays of vertically aligned multi-walled carbon nanotubes (VAMWCNTs) grown on the catalyst layer. Three arrays of VAMWCNTs may include a working electrode that may include a first array of VAMWCNTs, a reference electrode that may include a second array of VAMWCNTs, and a counter electrode that may include a third array of VAMWCNTs. In an exemplary implementation, the sensor may further include a passivation layer between the substrate and the catalyst layer.

In an exemplary implementation, the sensor may include one of a CNT based electrochemical chip similar to exemplary CNT based electrochemical chip **102** shown in FIG. **1**B, and a cancer diagnosis probe (CDP) similar to exemplary CDP **102** shown in FIG. **1**E. The substrate of the cancer CDP may include three needles, where each needle of the three needles may be coated by an array of VAMWCNTs of the three arrays of VAMWCNTs. In an exemplary implementation, the sensor may include exemplary sensor **102** as shown schematically in FIGS. **1**A, **1**B, and **1**E.

FIG. **2**B shows a schematic implementation of step **202** that may include putting the array of vertically aligned multi-walled carbon nanotubes (VAMWCNTs) grown on tip of each needle electrode of three needles electrodes **132**, **134**, and **138** of exemplary cancer diagnosis probe (CDP) **102** in contact with exemplary suspicious sample **250**, consistent with one or more exemplary embodiments of the present disclosure. Step **102** may include inserting or squeezing exemplary cancer diagnosis probe (CDP) **102** in exemplary suspicious sample **250**.

In an exemplary implementation, putting the array of VAMWCNTs of exemplary sensor **102** in contact with the suspicious sample may take place temporarily or over a time duration of less than 1 seconds for a real-time cancer diagnosis case. In an exemplary embodiment, putting the array of VAMWCNTs of exemplary sensor **102** in contact with the suspicious sample may take place temporarily or over a time duration of less than 1 seconds for in vivo or in vitro cancer diagnosis using exemplary sensor which may be an exemplary CDP or exemplary CNT based electrochemical chip. In an exemplary embodiment, putting the array of VAMWCNTs of exemplary sensor **102** in contact with the suspicious sample may be for a time duration of about 12 hours or more for in vitro cancer diagnosis cases with high levels of accuracy utilizing exemplary CNT based electrochemical chip **102**. In an exemplary embodiment, putting the array of VAMWCNTs of exemplary sensor **102** in contact with the suspicious sample may be carried out in a time duration of about 0.1 seconds to about 24 hours.

Step **204** may include recording the electrochemical response from the suspicious sample, where the electrochemical response may include an oxidation current peak. In an exemplary embodiment, the electrochemical response may include a cyclic voltammetry (CV) diagram of hypoxic glycolysis chemical reaction in biological cells within the suspicious sample. In an exemplary embodiment, the electrochemical response may include a cyclic voltammetry (CV) diagram of H_2O_2 related oxidation/reduction chemical reaction in biological cells within the suspicious sample. The concentration of H_2O_2 may be in correlation with the hypoxia glycolysis occurred in tumor cells. In an exemplary embodiment, the electrochemical response may include a cyclic voltammetry (CV) diagram of H_2O_2 oxidation that may be electrically sensed by VAMWCNTs in biological cells within the suspicious sample. In an exemplary embodiment, the electrochemical response may include an oxidation current peak of exemplary CV diagram of hypoxic glycolysis chemical reaction in biological cells within a suspicious sample.

In an exemplary implementation, recording the electrochemical response from the suspicious sample (step **204**) may include connecting the sensor to an electrochemical stimulator-analyzer, applying an electrical voltage on the sensor using the electrochemical stimulator-analyzer, and measuring the electrochemical response from the suspicious sample using the electrochemical stimulator-analyzer. In an exemplary embodiment, the electrochemical stimulator-analyzer may include a potentiostat.

Step **206** may include detecting the cancerous state in the suspicious sample responsive to a larger amount of the oxidation current peak than a threshold value. In an exemplary embodiment, the threshold value may include an oxidation current peak of about 700 μA or more when a time duration of putting the array of vertically aligned multi-walled carbon nanotubes (VAMWCNTs) of the sensor in contact with the suspicious sample (step **202**) may be more than about 12 hours. In an exemplary embodiment, the threshold value may include an oxidation current peak of about 80 μA or more when a time duration of putting the array of vertically aligned multi-walled carbon nanotubes (VAMWCNTs) of the sensor in contact with the suspicious sample (step **202**) may be about 5 seconds or less.

FIG. **2**C shows an implementation of detecting the cancerous state in the suspicious sample (step **206**), consistent with one or more exemplary embodiments of the present disclosure. Detecting the cancerous state in the suspicious sample (step **206**) may include recording a reference electrochemical response from a reference solution, where the reference electrochemical response may include a reference oxidation current peak (step **208**), comparing the electrochemical response with the reference electrochemical response (step **210**), and detecting the cancerous state in the suspicious sample responsive to a larger oxidation current peak of the electrochemical response in comparison with the reference oxidation current peak (step **212**). In an exemplary embodiment, the reference solution may include a lactate solution with a lactate concentration of about 0.05 mM or more.

In an exemplary implementation, electrochemical system **100** may be utilized for cancer diagnosis via exemplary method **200**. FIG. **3**A shows a schematic view of exemplary electrochemical reactions involved on sensor **102** including exemplary VAMWCNTs **130** as shown in FIGS. **1**D and **1**G, consistent with one or more exemplary embodiments of the present disclosure. Presence of H_2O_2 active molecule released during hypoxia glycolysis in a suspicious sample may be the main trigger of the electrochemical reactions. Hence, the chemical reaction occurring on the working electrode **108** including VAMWCNTs **130** may include:

$$L-\text{Lactate} + O_2 \xrightarrow[\text{Oxidase}]{L\text{-Lactate}} \text{Pyruvate} + H_2O_2 \qquad \text{Eq. 1}$$

$$H_2O_2 \rightarrow O_2 + 2H^+ + 2e^- \text{ response reaction of the } CDP \qquad \text{Eq. 2}$$

When the hypoxia glycolysis (Eq. 2) is activated (the concentration of O_2 is less than 5%) in cancer cells, increased reactive oxygen species (ROS) generated by mitochondria, would significantly enhance the cathodic peak of an electrochemical response measured from the suspicious sample which could be sharply detected by VAMWCNTs **130** electrodes. It may be known that the lactate released by hypoxic tumor cells during their glycolysis may not be discharged as a waste product, but may be taken up by oxygenated tumor cells as energy fuel in which Lactate is converted to pyruvate and H_2O_2 by LDH-B and then enters the mitochondria for OXPHOS to generate ATP. Similar to this process, the lactate released from hypoxic tumor cells may be used herein in electrochemical assay to trace the concentration of lactate due to the intensity of the H_2O_2 produced during LADH (Eq. 1) and released electrons due to the intensity of H_2O_2 oxidation reaction (Eq. 2).

FIG. **3**B shows a schematic overview of mitochondrial electron and proton fluxes in hypoxia, consistent with one or more exemplary embodiments of the present disclosure. During normaxia, electrons released from reduced cofactors (NADH and FADH2), flow through the redox centers of the respiratory chain (r.c.) to molecular oxygen (dotted lines), to which a proton flux from the mitochondrial matrix to the intermembrane space is coupled (grey arrows). Protons then flow back to the matrix through the F0 sector of the ATP synthase complex, driving ATP synthesis. ATP is carried to the cell cytosol by the adenine nucleotide translocator (grey arrows). Under moderate to severe hypoxia, electrons escape the r.c. redox centers and reduce molecular oxygen to the superoxide anion radical before reaching the cytochrome c (black arrows). Under these conditions, to maintain an appropriate Δψm, ATP produced by cytosolic glycolysis enters the mitochondria where it is hydrolyzed by the F1F0 ATPase with extrusion of protons from the mitochondrial matrix (black arrows). So, the mechanism of H_2O_2 detection by the VAMWCNTs **130** electrodes in hypoxia glycolysis may be based on released ion species during reduction of $NADH^+$, generation of ROS and production of superoxide anion radical by reducing molecular oxygen before reaching to cytochrome c. The amount of released charged species and increased current transferred by VAMWCNTs **130** electrodes may be correlated with the concentration of the lactate and subsequently H_2O_2 which resulted in ROS generated during hypoxia glycolysis.

Example 1: Fabrication of CNT Based Electrochemical Chip for In Vitro Assays

In this example, exemplary CNT based electrochemical chips was fabricated for in vitro assays. First, silicon wafer (p-type <100>) substrates were cleaned through standard RCA #1 method (NH_4OH:H_2O_2:H_2O solution and volume ratio of 1:1:5 respectively). Then, the cleaned substrates were rinsed in deionized (DI) water and dried by air. A thin layer of SiO_2 with a thickness of about 200 nm was grown by wet oxidation furnace on the surface of the silicon wafer, as a passivation layer. Nickel (Ni) catalyst layer for CNT growth with a thickness of about 9 nm was coated on SiO_2 by E-beam evaporation system at a temperature of about 120° C. with depositing rate of about 0.1 Angstroms/s. Afterwards, Ni-covered samples were located in a direct current plasma enhanced chemical vapor deposition (DC-PECVD) system to grow vertically aligned multi-walled carbon nanotubes (VAMWCNT). The growth process has three steps, including annealing, graining and growth. At first, the sample was annealed at a temperature of about 680° C. in an H_2 environment with a flow rate of about 35 standard cubic centimeters per minute (sccm) for about 30 minutes. During the graining, the surface was plasma hydrogenated for about 5 minutes with the intensity of about 5.5 $W \cdot cm^{-2}$ which results in the catalyst graining and formation of Ni nano-sized islands. In the growth step a plasma of C_2H_2 and H_2 mixture with flow rates of about 5 sccm and about 35 sccm were introduced to the chamber for about 15 minutes. Finally, CNT's were characterized with field emission scanning electron microscopy (FESEM). The length of CNTs ranged from about 2.5 to about 5 μm and the diameter of CNTs ranged from about 50 nm to about 70 nm.

FIG. **4** shows the FESEM image of the VAMWCNTs array on a portion of an exemplary fabricated CNT based electrochemical chip, consistent with one or more exemplary embodiments of the present disclosure. The CNTs were multi-walled carbon nanotubes with high purity and a presence of nickel on the top side of the CNTs could be related to the tip-growth mechanism. The CNT has been used as the work, counter and reference electrodes in exemplary fabricated CNT based electrochemical chips. The active area of the work, counter and reference electrodes were about 100 mm^2, 100 mm^2, 50 mm^2, respectively. The CNT based electrochemical chips were connected to a potentiostat by conductive wires bonded to the pads of the potentiostat.

Example 2: Fabrication of Cancer Diagnostic Probe (CDP) for In Vivo Assays

In this example, the tips of sterile steel needles were coated by Ni catalyst layers similar to that was described in EXAMPLE 1 for CNT based electrochemical chips with the assistance of E-Beam coating system. A fixture was designed and fabricated to hold the needles both in E-Beam and DC-PECVD systems to limit the growth of CNTs just in the tips of the needles. Then, the CNT grown needles were attached to electrical connectors with three pins by a conductive paste. Just tips of the needle were extended from the connectors up to about 1 cm. The probe was reinforced with a homemade holder and connected to a readout system by a noiseless cable which handled all three electrodes.

FIGS. **5A**-**5D** show FESEM images of a tip of a needle electrode of an exemplary fabricated cancer diagnostic probe (CDP) coated with an array of VAMWCNTs on the tip and exemplary portions **501**, **502** and **503** of the tip, consistent with one or more exemplary embodiments of the present disclosure. FIG. **5A** illustrates a FESEM image of the tip of a needle electrode of an exemplary fabricated cancer diagnostic probe (CDP) coated with the array of VAMWCNTs on the tip, consistent with one or more exemplary embodiments of the present disclosure. FIG. **5B** illustrates a FESEM image of portion **501** of the tip, consistent with one or more exemplary embodiments of the present disclosure. FIG. **5C** illustrates a FESEM image of portion **502** of the tip, consistent with one or more exemplary embodiments of the present disclosure. FIG. **5D** illustrates a FESEM image of portion **503** of the tip, consistent with one or more exemplary embodiments of the present disclosure.

Example 3: CV of H_2O_2 Contained Lactate Solution

In this example, the cyclic voltammetry (CV) diagram of L-lactic acid solution individually were recorded by exemplary electrochemical sensors including working electrodes (WEs) fabricated from platinum (Pt), Gold (Au), amorphous glassy carbon (GC) and carbon nanotube (CNT).

FIG. **6A** shows the CV diagrams of L-lactic acid solution individually recorded by electrochemical sensors fabricated from platinum (Pt) (curve **620**), Gold (Au) (curve **630**), amorphous glassy carbon (GC) (curve **640**), and carbon nanotube (CNT) working electrodes (WEs) (curve **650**), consistent with one or more exemplary embodiments of the present disclosure. It may be observed that the detected cathodic peak by CNT WE was so sharper (about 1500 μA) in similar concentration of H_2O_2 with respect to other electrodes (about 717, 5.7 and 0.8 μA in Au, Pt and GC electrodes, respectively). CNT greatly transfer the released charges from oxidized H_2O_2 beneath the nanotubes in media solution. Hence, CNT arrays were used as electrodes of exemplary sensors in the present disclosure.

FIG. **6B** shows the CV diagrams of solutions with various concentrations of lactate (and subsequently H_2O_2) recorded by electrochemical sensors with CNT arrays working electrode, consistent with one or more exemplary embodiments of the present disclosure. CV diagrams were recorded for solutions with a lactate concentration of about 0.025 mM (CV diagram **602**), 0.05 mM (CV diagram **604**), 0.1 mM (CV diagram **606**), and 0.3 mM (CV diagram **608**). CNT working electrode presented a well concentration depended increased response to the presence of lactate molecules in the solutions ranged from about 0.025 mM (CV diagram **602**) to about 0.3 mM (diagram **608**).

FIG. **6C** shows the CV diagrams of H_2O_2 contained lactate solution with a lactate concentration of about 0.3 mM (CV diagram **614**) in comparison with two cell culture solutions RPMI (CV diagram **610**) and DMEN (CV diagram **612**) recorded by electrochemical sensors with CNT arrays working electrode, consistent with one or more exemplary embodiments of the present disclosure. It may be observed that RPMI and DMEN cell culture solutions show less electrochemical responses in comparison with H_2O_2 contained lactate solution. The RPMI presented no electrochemical responses in the voltage attributed to the lactate detection. As a result, RPMI could be applied as cellular and tissue culture media with a negligible false positive response.

Example 4: Electrochemical Responses of Different Cell Lines

In this example, electrochemical sensing of H_2O_2 produced during Lactate/Pyruvate hypoxic glycolysis was verified in four different phenotypes of breast cell lines ranged from normal to malignant stages, including: MCF10 A, MCF-7, MDA-MB-231, and MDA-MB-468. Breast cancer cell lines (MCF10A, MCF-7, MDA-MB-231, MDA-MB-468) were obtained and were maintained at 37° C. (5% CO_2, 95% air) in RPMI medium supplemented with 5% fetal bovine serum, and 1% penicillin/streptomycin. The fresh medium was replaced every other day. All cell lines were tested and found negative for *Mycoplasma* contamination. The cells were detached from the plates by trypsin and counted by neobar laam.

FIG. **7** shows the CV responses of normal (MCF10A: CV diagram **702**) and different grades of cancerous (MCF7: CV diagram **706**, MDA-MB231: CV diagram **708**, and MDA-B468: CV diagram **710**) breast cells' solution media cultured for about 48 hours in comparison with standard H_2O_2 contained lactate solution with a lactate concentration of about 0.3 mM (CV diagram **712**) and RPMI (CV diagram **704**) in individual sensing wells of exemplary fabricated sensor in EXAMPLE 1 herein above, consistent with one or more exemplary embodiments of the present disclosure. Lactate production due to hypoxic glycolysis would be well detectable after about 48 hours of incubation in cancer cell lines. The CV diagrams of FIG. **7** show that the intensity of oxidation peak, located at the position of H_2O_2 electrochemical response, significantly increased with the progression in invasive grades of cancer cells in which hypoxia glycolysis would be enhanced.

Referring to FIG. **6B** and FIG. **7**, sharp difference in electrochemical peaks of H_2O_2 contained lactate solution was observed from about 0.025 mM to about 0.05 mM which could be applied to calibrate cancer cells' media from normal ones. Because the electrochemical responses of cancer cells' media solution was equal to the response range of H_2O_2 contained lactate solution with the concentration of more than about 0.05 mM meanwhile such response in normal cells was equal to the response range of the H_2O_2 contained lactate solution with the concentration of less than about 0.025 mM.

Moreover, similar responses were recorded from the culture media of colon, prostate, liver, lung, mouth, neural and hematopoietic cell lines in normal and cancer phenotypes with invasive and moderate grades by electrochemical sensing of H_2O_2 produced during Lactate/Pyruvate hypoxic glycolysis for some other types of colon, neural, prostate, liver, mouth, hematopoietic and lung cell lines. Colon (COR-L 105, SW-480, HT-29), Hematopoietic (1301, LCL-PI 1), Liver (HEP G2), Lung (QU-DB, MRC-5), Mouth (KB), Neuron (BE(2)-C, LAN-5), Prostate (PC-3, Du-145) cell lines were obtained and were maintained at 37° C. (5% CO_2, 95% air) in RPMI medium supplemented with 5% fetal bovine serum, and 1% penicillin/streptomycin. The fresh medium was replaced every other day. All cell lines were tested and found negative for *Mycoplasma* contamination. The cells were detached from the plates by trypsin and counted by neobar laam.

FIGS. **8**A-**8**G shows the CV responses of the solution media of different normal and cancerous cell lines in various phenotypes including Colon (COR-L 105 **802**, SW-480 **803**, HT-29 **804**) in FIG. **8**A, Hematopoietic (1301 **805**, LCL-PI 1 **806**) in FIG. **8**B, Liver (HEP G2 **807**) in FIG. **8**C, Lung (QU-DB **808**, MRC-5 **809**) in FIG. **8**D, Mouth (KB **810**) in FIG. **8**E, Neuron (BE(2)-C, LAN-5) in FIG. **8**F, and Prostate (PC-3 **813**, Du-145 **814**) in FIG. **8**G cell lines in comparison with Reference diagram **801** for H_2O_2 contained lactate solution with a lactate concentration of about 0.3 mM, consistent with one or more exemplary embodiments of the present disclosure. The current peaks in cancerous samples were observably increased. The H_2O_2 based oxidative peaks of cancer media solutions were sharper than that in normal cells. Grade dependent increase was observed in H_2O_2 peaks of cancer cells with sharp difference between normal and cancer phenotypes in all of the cell lines. This reveal the increased hypoxia glycolysis in cancer cells with respect to that in normal cells. A great correlation was observed between the cells' phenotypes and their lactate based H_2O_2 electrochemical responses.

Example 5: In Vitro Diagnosis of Cancer in Samples by Electrochemical Tracking of Hypoxia Glycolysis in Secretion of the Samples

In this example, the electrochemical responses of 6 breast tissues removed by biopsy (core needle biopsy (CNB)) or surgery from 6 of suspicious patients to cancer were analyzed using exemplary CNT based electrochemical chip. The size of the removed samples was similar (with the non-dehydrated weight of about 25 mg). The electrochemical responses were compared with cytopathological analysis done by Hematoxylin and Eosin (H & E) staining of the 6 breast tissues. Each resected sample was maintained in RPMI for about 24 hours before analyzing by exemplary CNT based electrochemical chip to be ensured from the lactate release in hypoxic tumors. Before pathological assaying, each resected sample was fixed in Formaline. For electrochemical analysis of hypoxia glycolysis in secretion of the samples, live spices from CNB or surgically removed samples were cut in similar specimens and directly transferred through sensing wells of exemplary CNT based electrochemical chip containing RPMI-1640 without any preprocessing. About 24 hours after maintaining the samples in incubator, about 200 μl of the culture media was dropped to individual sensing wells and the cathodic current of electrochemical responses of H_2O_2 were recorded in CV profile.

FIGS. **9**A-**9**F show the cytopathological results (H&E images) (top side) and electrochemical responses (bottom side) of the breast tissues removed by biopsy or surgery from 6 suspicious patients to cancer, consistent with one or more exemplary embodiments of the present disclosure. The electrochemical responses were calibrated based on the reference H_2O_2 contained lactate solution with a lactate concentration of about 0.3 mM as used for cell lines in EXAMPLE 4 above. The intensity of oxidation peak and released electrons strongly correlated to the lactate produced by hypoxia glycolysis in cancer cells. A well correlation could be observed between increased H_2O_2 dependent current peak and cancer transformed morphology of the tissues. A great match observed between the quantified electrochemical response and pathological result of the samples in which the normal and hyperplasic tissues expressed low levels of H_2O_2 related current peak meanwhile the cancerous tissues exhibited high levels of H_2O_2 related electrochemical peaks. Accordingly, FIGS. **9**A-**9**C show results obtained from non-cancerous samples and FIGS. **9**D-**9**F show results obtained from cancerous samples.

Similar electrochemical responses of 5 more samples, including live spices from CNB or surgically removed samples, were obtained using exemplary CNT based electrochemical chip. FIG. **10** shows a columnar diagram of electrochemical responses of the breast tissues removed by biopsy or surgery from 11 suspicious patients to cancer, consistent with one or more exemplary embodiments of the present disclosure. Referring to this figure, two regimes **1002** and **1003** of responses were achieved due to the trace of hypoxia glycolysis based on LADH in comparison with a reference state **1001** of a H_2O_2 contained lactate solution with a lactate concentration of about 0.3 mM. In regime 1 indicated by **1002**, the oxidation peaks were ranged from about 933.9 μA to about 1068.9 μA, and in regime 2 indicated by **1003**, the oxidation peaks were ranged from about 269.6 μA to about 718 μA. The pathological results showed a well correlation with this determination. The samples presented high levels of hypoxia related oxidative peaks (categorized in regime 1) were verified as cancer in their H&E assays. Nests of distinguished tumoral cells in H&E images of those patients could be observed in FIGS. **9**D-**9**F. Such responses were observed in the H_2O_2 contained lactate solution with the concentration of more than about 0.05 mM (FIG. **6**B). Samples with low levels of lactate (regime2) were diagnosed as non-cancer with different types of benign cancer patients such as hyperplasia (peak: 556.5 μA) in FIG. **9**B, lactational changes (peak: 718 μA), and so on. These electrochemical responses were equal to the peak determined in H_2O_2 contained lactate solution with the concentration of less than about 0.025 mM (FIG. **6**B). Comparative columnar diagram presented in FIG. **10** would elaborate the difference in lactate based electrochemical response between normal and cancer tissues.

Example 6: Standard Colorimetric Lactate Assay Kit

As the released H_2O_2 concentration have a direct correlation with lactate concentration, to further investigate the accuracy of exemplary electrochemical method described above, the results of both cell lines (described in EXAMPLE 4) and patients' samples (described in EXAMPLE 5) were compared by standard colorimetric lactate assay kit. Although this method is so time consuming and expensive with complicated multi sequential steps, it was conducted to check the reliability of lactate concentration based cancer diagnosis measured by exemplary CNT based electrochemical chip. Comparative responses versus reference H_2O_2 contained lactate solution for both electrochemical and Lactate Kit assays are presented in Table 1 and Table 2.

TABLE 1

Comparative responses of CNT based electrochemical chip and standard Lactate Kit Assay on 4 different phenotypes of Breast cell lines.

Cell line	Electrochemical sensor: Relative Current (%)	Lactate kit: Relative Lactate Concentration (%)
Reference lactate solution	100	100
MCF 10A	31.1	31.1
MCF-7	52.9	56.3
MDA-MB-231	69.5	70.9
MDA-MB-468	91.5	91.5

TABLE 2

Diagnostic results of 11 patients suspicious to breast cancer determined by H&E, Lactate kit, and the cathodic peaks of released H_2O_2 from the cells measured by CNT based electrochemical chip assays, respectively.

Patient ID	Type of Tissue	H & E Result	Lactate Kit Result (%)	CNT Electrochemical Sensor (%)
Reference lactate solution	—	—	100	100
1	Normal	Non Cancer	22.2	22.2
2	Normal	Left Hyper Plasy	42.3	42.3
3	Normal	Lactational Change	59.1	59.2
4	Normal	Adenosis benign glandular prolifration	53.8	53.7
5	Normal	Hyperplasy and inflammation	45.9	45.9
6	Suspicious to Cancer	Lympho vascular invasion	88.1	88.2
7	Suspicious to Cancer	Cancer	77.2	77.2
8	Suspicious to Cancer	Cancer	85.5	85.4
9	Suspicious to Cancer	Cancer	80.5	80.5
10	Suspicious to Cancer	Cancer	85.1	85.2
11	Suspicious to Cancer	Cancer	62	62.2

A correlation was observed between the responses of the CNT based electrochemical chip and kit which revealed the accuracy of CNT based electrochemical chip in lactate based cancer detection as shown in Table 1 and Table 2. The raw values recorded by Lactate kit and electrochemical sensing wells were presented in these tables. In summary, tracing the hypoxia glycolysis (correlated with lactate concentration) in the interstitial fluid of biopsy sample by electrochemical assay with suitable electrode (such as CNT) exhibited a high correlation with their pathological states and may be used as a new method in cancer diagnosis.

Example 7: Integrated Assay on the Tip of the Needles of Cancer Diagnostic Probe (CDP) for Real-Time Cancer Detection Both In Vitro and In Vivo

To extend the application of exemplary label free electrochemical method of the present disclosure in real-time and precise detection of the tumor tissues during interventional sonography or surgery, exemplary CDP fabricated by growth of carbon nanostructures on the tip of the sterile steel needles as described in EXAMPLE 2 was used herein. Such integrated system contains three carbonated needles as working electrode (WE), counter electrode (CE), and reference electrode (RE). The needles were rinsed by PBS, Ethanol 70% and DI water followed by drying in N_2 ambient and UV sterile to prevent from any detachment and remaining the residues of the nanotubes in the tissue. CV responses were taken immediately after squeeze of exemplary CDP into the breast cancerous and normal tissues that indicated sharp increase in the current peak of the CDP with CNT covered electrodes interacted by cancer tissue. The important point is that the diagnosis was completed in live time based on monitoring the lactate concentration of the tissues inner domain.

FIG. **11**A shows CV response of exemplary CDP with all three needles covered by VAMWCNTs immediately after connection to the tissues, consistent with one or more exemplary embodiments of the present disclosure. It may be observed that reversible shapes with symmetric anodic and catholic peaks were obtained in CV responses. Distinguishable response between normal and cancer tissues may be observed.

FIG. **11**B shows CV response of exemplary CDP with only working electrode covered by VAMWCNTs immediately after connection to the tissues, consistent with one or more exemplary embodiments of the present disclosure. Quality of the peaks were degraded when replacing the RE and CE by steel needle. The intensity and symmetry of the responses were degraded in the sensor with just CNT covered WE (CE and RE were steel needles).

FIG. **11**C shows CV response of exemplary CDP with non-CNT covered by needles immediately after connection to the tissues, consistent with one or more exemplary embodiments of the present disclosure. There may be observed a noisy response without any distinguishable electrochemical peak. When all of the electrodes were non CNT covered needles, the responses were completely degraded and not distinguishable between normal and cancer tissues. This revealed the important role of CNT in selective interaction and charge transfer from the H_2O_2 released during transformation of lactate to pyruvate.

FIGS. **12**A-**12**E show CV responses recorded by exemplary CDP (needle based electrochemical sensor) from the resected tissues from five patients among 50 individual patients suspicious to breast cancer at the bottom side of FIGS. **12**A-**12**E in comparison with images obtained by conventional pathological methods (H&E) at the top side of FIGS. **12**A-**12**E, consistent with one or more exemplary embodiments of the present disclosure. Patients respective to FIGS. **12**A-**12**C have normal/non-cancerous (FIG. **12**A), hyperplasic (FIG. **12**B), and adenosis glandular proliferative tissues (FIG. **12**C). Patients respective to FIGS. **12**D and **12**E have cancer tissues. Electrochemical current peaks of cancer tissues are sharply (more than about 150 μm) higher than benign ones with a strong correlation by the abundance of distributed cancer cells. The CV responses recorded from the normal and cancer tissues of these 50 individual patients by CNT covered needle sensors (CDP) greatly detected the hypoxic glycolysis just in cancerous samples due to cathodic peaks of H_2O_2 (FIGS. **12**A-**12**E). Meanwhile, while the response time of CDP was less than about 1 minute after the tissue resection, diagnosis by conventional pathological methods (H&E) requires at least several hours for sample fixation and staining procedures. The ratio of cathodic peaks of reference H_2O_2 contained lactate solution vs. non-cancerous tissues were more than three times (FIGS. **12**A-**12**C) while such ratio was less than one time in cancerous tissues (FIGS. **12**D and **12**E).

Table 3 shows the results recorded by exemplary CDP in comparison with the results obtained by H&E analysis from live resected tissues of 50 patients suspicious to breast cancer. They exhibited great correlations with the pathological results of the samples assayed by H&E method.

TABLE 3

Results recorded by exemplary CDP in comparison with the results obtained by H&E analysis from live resected tissues of 50 patients suspicious to breast cancer.

Patient ID	Oxidation Current Peaks (μA)	CDP (Cancer)	H&E (Cancer)
1	0	Negative	NO
2	46.6	Negative	NO
3	87	Negative	NO
4	316.5	Positive	YES (Cancer 90%, Normal 10%)
5	287.8	Positive	YES (Cancer 90%, Normal 10%)
6	22	Negative	NO
7	142.3	Positive	YES (Cancer 30%, Normal 70%)
8	150	Positive	YES (Cancer 30%, Normal 70%)
9	300	Positive	YES (Cancer 90%, Normal 10%)
10	13	Negative	NO
11	0	Negative	NO
12	101.5	Positive	YES (Cancer 30%, Normal 70%)
13	180.2	Positive	YES (Cancer 60%, Normal 40%)
14	289.4	Positive	YES (Cancer 90%, Normal 10%)
15	302	Positive	YES (Cancer 90%, Normal 10%)
16	274.2	Positive	YES (Cancer 90%, Normal 10%)
17	0	Negative	NO
18	142.8	Positive	YES (Cancer 30%, Normal 70%)
19	80	Negative	NO
20	32.5	Negative	NO
21	200	Positive	YES (Cancer 60%, Normal 40%)
22	188.2	Positive	YES (Cancer 60%, Normal 40%)
23	264.5	Positive	YES (Cancer 90%, Normal 10%)
24	23	Negative	NO
25	179.5	Positive	YES (Cancer 60%, Normal 40%)
26	55.2	Negative	NO
27	52	Negative	NO
28	77	Negative	NO
29	0	Negative	NO
30	201	Positive	YES (Cancer 60%, Normal 40%)
31	75.6	Negative	NO
32	155.8	Positive	YES (Cancer 30%, Normal 70%)
33	99.5	Positive	YES (Cancer 30%, Normal 70%)
34	305.5	Positive	YES (Cancer 90%, Normal 10%)
35	297.7	Positive	YES (Cancer 90%, Normal 10%)
36	112	Positive	YES (Cancer 30%, Normal 70%)
37	17.8	Negative	NO
38	40	Negative	NO
39	73	Negative	NO
40	290	Positive	YES (Cancer 90%, Normal 10%)
41	90	Positive	YES (Cancer 30%, Normal 70%)
42	330	Positive	YES (Cancer 90%, Normal 10%)
43	197.5	Positive	YES (Cancer 30%, Normal 70%)
44	77.5	Negative	NO
45	25	Negative	NO
46	266.2	Positive	YES (Cancer 90%, Normal 10%)
47	0	Negative	NO
48	102.5	Positive	YES (Cancer 30%, Normal 70%)
49	310	Positive	YES (Cancer 90%, Normal 10%)
50	259.3	Positive	YES (Cancer 90%, Normal 10%)

FIG. **13** shows a summary of categorized regimes of CV responses recorded by exemplary CDP from the resected tissues from five patients among 50 individual patients suspicious to breast cancer that were presented in Table 3. It represents CV regimes along a spectrum from a completely non-cancerous state to cancerous state, consistent with one or more exemplary embodiments of the present disclosure. It may be seen that if the H_2O_2 cathodic peak (equal to oxidation current peak) of exemplary CV response recorded by exemplary CDP from a patient is less than 90 μA, the tissue is in non-cancerous state. On the other hand, if the CV response recorded by exemplary CDP from the tissue is in a range more than about 95 μA, there exists a cancerous state which may be more intensified by increasing the oxidation current peak. A range of oxidation current peak between 90 μA and 95 μA is the border range.

Example 8: In Vivo Analysis of Observable Tumor with Histologically Distinct Cancer Margin Before any Mastectomy

To determine if CDP would in real time identify an observable tumor in vivo, about 2.3×10^6 4T1-derived cancer cells were implanted into the back of 10 female BALB/C mice, and the mice were maintained in individual groups with similar size of formed tumors with sharp histologically distinct patterns. After about 10 days, individual CDPs were externally squeezed into their cancerous and normal regions had been specified by sonography. The space between each assayed regions was about 3 mm. Also the mice under body were connected to ground potential such as done for any patient in surgery room.

FIG. **14**A shows a sonography image from a tumor side taken from an exemplary mouse tumorized by 4T1 breast cancer cell lines, consistent with one or more exemplary embodiments of the present disclosure. A tumor with average sizes with a length **1402** of about 2.24 cm and another length **1404** of about 1.60 cm could be observed in sonography image.

FIG. **14**B shows H&E image from the tumor side taken from exemplary tumorized mouse by 4T1 breast cancer cell lines, consistent with one or more exemplary embodiments of the present disclosure. FIG. **14**C shows H&E image from a normal/healthy side taken from exemplary tumorized mouse by 4T1 breast cancer cell lines, consistent with one or more exemplary embodiments of the present disclosure.

FIG. **14**D shows CV diagrams of normal and tumor regions/sides of exemplary tumorized mouse by 4T1 breast cancer cell lines calibrated by a Reference CV diagram from H2O2 contained lactate solution with a lactate concentration of about 0.3 mM obtained using exemplary CDP, consistent with one or more exemplary embodiments of the present disclosure. It may be observed that the lactate related peaks were about 3 times higher in cancer region (CV diagram **1406** and FIGS. **14**A and **14**B) versus normal ones (CV diagram **1408** and FIG. **14**C). Sharp lactate electrochemical peaks were observed in tumor locations by about three times higher current than that recorded from their normal regions

To more clearly clarify the impact of H_2O_2 monitoring in tumor growth and progression, tumor size effects on H_2O_2 related electrochemical peaks recorded by CDP were compared. A distinguishable increasing regime was observed in the intensity of current peak through increment in the tumor size. Moreover, Histopathological images taken from the normal and cancer regions detected by CDP confirmed this result. Hyper chromatic and irregular nucleus with increased nucleus/cytoplasm ratio may be observable in H&E images of cancer region.

Example 9: In Vivo Analyses of Suspicious Regions Before and During the Surgery

In this example, the ability of the CDP to distinguish suspicious regions to cancer in mice model was analyzed by the resolution of about 3 mm which could be translated to human model. Tissue samples that contained regions of invasive breast cancer adjacent to normal stroma were experimented.

Five tumorized mice by 4T1 breast cancer cell lines were checked by sonography. FIG. **15**A shows a sonography image from a tumor **1501** taken from an exemplary mouse tumorized by 4T1 breast cancer cell lines, consistent with one or more exemplary embodiments of the present disclosure. Approximate dimensions of the tumor could be observed in sonography image of FIG. **15**A.

Exemplary CDP was tested on tumor and suspicious regions of the five tumorized mice before (by squeezing through skin) and during the surgery on exemplary six regions. FIGS. **15**B and **15**C show exemplary six analyzed regions **1502**-**1507** of an exemplary tumorized mouse among the exemplary five tumorized mice before (FIG. **15**B) and during surgery (FIG. **15**C), consistent with one or more exemplary embodiments of the present disclosure. Six analyzed regions may include center **1502** of tumor **1501**, left side **1503** of tumor **1501**, right side **1504** of tumor **1501**, upside **1505** of tumor **1501**, bottom side **1506** of tumor **1501**, and also an exemplary normal side **1507** far from tumor **1501** all depicted in FIGS. **15**B and **15**C were analyzed consecutively before and during surgery using a CDP with an about 3 mm distance between needle electrodes.

Moreover, frozen H&E assay was used and rechecked by IHC method to be ensure from the precision of CDP results with respect to standard protocols. A tissue section of the sample including exemplary six regions analyzed by exemplary CDP was subjected to frozen H&E staining processes and evaluated by the pathologist. Exemplary tumor **1501** containing suspicious regions was removed and sent for frozen pathology and the H&E images taken from the center **1502** of tumor **1501** as well as its posterior **1505**, anterior **1506**, right **1504** and left **1503** laterals with the distance of about 3 mm from the histologically distinct region, were demanded by the CDP results as presented in Table 4. The results of CDP before and during surgery exhibited a perfect correlation. Ki67 based IHC assay confirmed the normal state of R5 and cancer involvement in R3 as classifier reference.

TABLE 4

Results recorded by exemplary CDP before and during surgery in comparison with the results obtained by H&E analysis from six suspicious regions of an exemplary tumorized mouse.

Region	CDP Before Surgery (Ox Current Peaks (μA))	CDP During Surgery (Ox Current Peaks (μA))	H&E frozen (Cancer)
1502 (Center)	Positive (169.104)	Positive (178.621)	Yes (Cancer 90%, Normal 10%)
1503 (Right)	Positive (94.773)	Positive (96.89)	Yes (Cancer 30%, Normal 70%)
1504 (Left)	Positive (122.643)	Positive (122.8)	Yes (Cancer 60%, Normal 40%)
1505 (Up)	Negative (30.397)	Negative (31.85)	No
1506 (Bottom)	Negative (0)	Negative (0)	No
1507 (Normal)	Negative (0)	Negative (0)	No

As represented in Table 4, it was distinguished from H&E analyzes that center **1502** was diagnosed by frozen histopathology as cancer tissue, whereas regions **1505** and **1506** were diagnosed as normal stroma. Region **1504** was in the margin between the cancer and normal stroma tissue regions, presenting about 40% tumor tissue and about 60% normal stroma tissue. Region **1503** was a suspicious region without any tumor margins but the trace of distributed cancer cells would be observed between stroma. Tumoral cells would be distinguished due to their hyper chromic nuclei (triangular arrows in H&E images of regions **1503** and **1504**). Tabled result shows the CDP obtained for regions **1502** and **1504** presented significant hypoxic lactate peaks meanwhile lower but detectable meaningful levels of the H_2O_2 was recorded for region **1503**. No detectable trace of any peak was measured for region **1506**. The CDP response obtained for **1507**, diagnosed as reference normal stroma tissue, presented no H_2O_2 peak similar to that observed for **1506**.

The CDP response obtained for regions **1504** and **1506** were then evaluated by Ki67 IHC as an independent validation set. The expression of Ki67 has been reported to be correlated with tumor cell proliferation and growth in routine pathological investigation and used as a diagnostic marker. Ki67 based IHC classifier identified no trace of cancer proliferation in region **1506** (as the normal stroma) and showed different intensities of filtrated cancer cells in region **1504**. Similar results were obtained for 5 other animal models with suspicious regions in anterior, posterior, right and left laterals of their tumors.

In addition, exemplary CDP exhibited a fine distinguishable response in interaction with another type of cancer tumors (MC4L2) as cancer cells with lower invasive grades than 4T1 as experimented on mice models. Tumors formed by the injection of about 5×10^5 MC4L2 cells (mice primary breast cancer cell lines) were analyzed by exemplary CDP on 5 mice.

FIG. **16** shows comparative diagram of CDP responses in interaction with normal (curve **1601**), non-metastasized tumor (curve **1602**) and metastatic tumor (curve **1603**) recorded from individual mice, consistent with one or more exemplary embodiments of the present disclosure. Tracing the hypoxia glycolysis exhibited a strong correlation with the invasive state of the tumor. Results revealed sharply distinguishable responses between cancerous and normal regions. However the intensity of the response of MC4L2 tumors is lower than that was recorded for malignant tumor, it is observably higher than the response peak of normal tissue.

Furthermore, in this example, exemplary CDP was applied in finding the suspicious margins during tumor resection surgery in breast cancer patients. Not only the known normal domains were detected and set as reference point, but also suspicious margins of cancer and normal domains were precisely diagnosed in real-time and confirmed by histopathological assays. So, without requirement to frozen pathological process the surgeon can finish the surgery with insurance from precise resection of tumor without any additional mastectomy from the peripheral tissues.

FIGS. **17A-17C** shows CV responses obtained by applying exemplary CDP in detection of suspicious margins during breast cancer surgery for a known normal region (FIG. **17A**) that was checked as calibrating data, and two suspicious margins (FIGS. **17B** and **17C**) that were precisely diagnosed as cancerous (FIG. **17B**) and normal (FIG. **17C**) domains by CDP in real-time, consistent with one or more exemplary embodiments of the present disclosure. The results obtained by exemplary CDP were confirmed by H&E analysis. FIGS. **17D-17F** shows H&E results after the surgery for the known normal region, and two suspicious margins, consistent with one or more exemplary embodiments of the present disclosure.

These results show that the diagnostic information obtained by exemplary CDP can be used to detect cancer in marginal suspicious regions with rare distribution of cancer cells filtrated between normal stroma in less than about 20 seconds during the surgery or biopsy of live animal as well as human models without any requirement to tissue resection and preparation for frozen pathology. Even it may detect the accurate location of cancer involved regions before surgery in superficial tumors. The precision of this method is as well as reported for H&E from the assayed regions.

While the foregoing has described what are considered to be the best mode and/or other examples, it is understood that various modifications may be made therein and that the subject matter disclosed herein may be implemented in various forms and examples, and that the teachings may be applied in numerous applications, only some of which have been described herein. It is intended by the following claims to claim any and all applications, modifications and variations that fall within the true scope of the present teachings.

Unless otherwise stated, all measurements, values, ratings, positions, magnitudes, sizes, and other specifications that are set forth in this specification, including in the claims that follow, are approximate, not exact. They are intended to have a reasonable range that is consistent with the functions to which they relate and with what is customary in the art to which they pertain.

The scope of protection is limited solely by the claims that now follow. That scope is intended and should be interpreted to be as broad as is consistent with the ordinary meaning of the language that is used in the claims when interpreted in light of this specification and the prosecution history that follows and to encompass all structural and functional equivalents. Notwithstanding, none of the claims are intended to embrace subject matter that fails to satisfy the requirement of Sections 101, 102, or 103 of the Patent Act, nor should they be interpreted in such a way. Any unintended embracement of such subject matter is hereby disclaimed.

Except as stated immediately above, nothing that has been stated or illustrated is intended or should be interpreted to cause a dedication of any component, step, feature, object, benefit, advantage, or equivalent to the public, regardless of whether it is or is not recited in the claims.

It will be understood that the terms and expressions used herein have the ordinary meaning as is accorded to such terms and expressions with respect to their corresponding respective areas of inquiry and study except where specific meanings have otherwise been set forth herein. Relational terms such as first and second and the like may be used solely to distinguish one entity or action from another without necessarily requiring or implying any actual such relationship or order between such entities or actions. The terms “comprises,” “comprising,” or any other variation thereof, are intended to cover a non-exclusive inclusion, such that a process, method, article, or apparatus that comprises a list of elements does not include only those elements but may include other elements not expressly listed or inherent to such process, method, article, or apparatus. An element proceeded by “a” or “an” does not, without further constraints, preclude the existence of additional identical elements in the process, method, article, or apparatus that comprises the element.

The Abstract of the Disclosure is provided to allow the reader to quickly ascertain the nature of the technical disclosure. It is submitted with the understanding that it will not be used to interpret or limit the scope or meaning of the claims. In addition, in the foregoing Detailed Description, it can be seen that various features are grouped together in various implementations. This is for purposes of streamlining the disclosure, and is not to be interpreted as reflecting an intention that the claimed implementations require more features than are expressly recited in each claim. Rather, as the following claims reflect, inventive subject matter lies in less than all features of a single disclosed implementation.

Thus, the following claims are hereby incorporated into the Detailed Description, with each claim standing on its own as a separately claimed subject matter.

While various implementations have been described, the description is intended to be exemplary, rather than limiting and it will be apparent to those of ordinary skill in the art that many more implementations and implementations are possible that are within the scope of the implementations. Although many possible combinations of features are shown in the accompanying figures and discussed in this detailed description, many other combinations of the disclosed features are possible. Any feature of any implementation may be used in combination with or substituted for any other feature or element in any other implementation unless specifically restricted. Therefore, it will be understood that any of the features shown and/or discussed in the present disclosure may be implemented together in any suitable combination. Accordingly, the implementations are not to be restricted except in light of the attached claims and their equivalents. Also, various modifications and changes may be made within the scope of the attached claims.

What is claimed is:

1. An electrochemical system for cancer diagnosis, comprising:

a sensor configured to be put in contact with a sample suspected of being cancerous, the sensor comprising:

a working electrode;

a reference electrode; and

a counter electrode,

wherein each of the working electrode, the reference electrode and the counter electrode comprise an array of vertically aligned multi-walled carbon nanotubes (VAMWCNTs), the VAMWCNTs configured to be put in direct contact with the sample, and

wherein the sensor comprises a carbon nanotube (CNT) based electrochemical chip comprising at least one sensing well, the at least one sensing well comprising:

a substrate;

a passivation layer grown on the substrate; and

a catalyst layer coated on the passivation layer, wherein each of the arrays of VAMWCNTs are grown on the catalyst layer within the at least one sensing well, wherein the at least one sensing well is configured for placement of the sample thereon;

an electrochemical stimulator-analyzer, the electrochemical stimulator-analyzer configured to:

electrochemically stimulate the sample in contact with the sensor by applying an electrical voltage to the sensor; and

measure Hydrogen Peroxide (H_2O_2) oxidation during a hypoxic glycolysis chemical reaction within the sample by measuring an electrochemical response from the sensor, the electrochemical response comprising an oxidation current peak;

a processor electrically connected to the electrochemical stimulator-analyzer, the processor configured to:

control an electrochemical stimulation of the sample in contact with the sensor utilizing the electrochemical stimulator-analyzer;

receive the measured electrochemical response from the electrochemical stimulator-analyzer;

record the measured electrochemical response; and

determine a cancerous state of the sample by analyzing the measured electrochemical response, comprising:

comparing the oxidation current peak of the measured electrochemical response with a reference oxidation current peak of 700 μA; and

determining the sample to be cancerous with a breast cancer if the oxidation current peak is larger than the reference oxidation current peak; and

an array of electrically conductive connectors, the sensor connected to the electrochemical stimulator-analyzer via the array of electrically conductive connectors.

2. The electrochemical system of claim **1**, wherein the substrate comprises at least one of a silicon chip and a silicon wafer.

3. The electrochemical system of claim **1**, wherein the passivation layer comprises a layer of SiO_2 with a thickness of less than 500 nm.

4. The electrochemical system of claim **1**, wherein the catalyst layer comprises a layer of Nickel (Ni) with a thickness of less than 10 nm.

5. The electrochemical system of claim **1**, wherein the electrochemical response comprises a cyclic voltammetry (CV) diagram with the oxidation current peak of the hypoxic glycolysis chemical reaction in biological cells within the sample.

6. The electrochemical system of claim **1**, wherein the electrochemical stimulator-analyzer comprises a potentiostat.

7. The electrochemical system of claim **1**, wherein the sample comprises one of a liquid suspected sample, a solid suspected sample, and combinations thereof.

8. The electrochemical system of claim **1**, wherein the sample comprises one of a plurality of cell lines, a biopsied sample from a human or animal body, a sample removed from a human or animal body by surgery, a portion of a living tissue in a human or animal body, and a portion of a living tissue in a human or animal body during surgery.

* * * * *